Review

Exploring Molecular Aspects of Cardiovascular Diseases on Animal Models

Dumitru A. Iacobas * and Dennis Daniels

Posted Date: 5 May 2026

doi: 10.20944/preprints202605.0124.v1

Keywords: chagas disease; chamber transcriptomic specificity; hypoxia; low-salt diet; metabolic syndrome; sex dichotomy; post-ischemic heart failure; pulmonary hypertension

 doi:10.20944/preprints202605.0124.v1

Review

Exploring Molecular Aspects of Cardiovascular Diseases on Animal Models

Dumitru A. Iacobas * and Dennis Daniels

Undergraduate Medical Academy, School of Public and Allied Health, Prairie View A&M University, Prairie View, TX 77446, USA

* Correspondence: daiacobas@pvamu.edu

Abstract

Despite the wide palette of clinically available investigative tools, not all deep molecular phenomena governing the cardiovascular system can be studied on living humans. Therefore, a reasonable alternative is to explore such phenomena on animal models, given that the two-circuits centered on a tetra chamber heart practically did not evolve since the crocodilians. This review presents our two decades-long experience with mouse, rat and dog models of Chagas disease, metabolic syndrome, post ischemic heart failure, and pulmonary hypertension. We studied also the transcriptomic consequences of cell treatment of Chagas and ischemic cardiomyopathies, genetic engineering, and exposure to hypobaric hypoxia, oxygen deprivation, low salt and high fructose diets. Among others, the investigations revealed heart transcriptomic sex dichotomy and inter-chamber differences, as well as changes in the subcellular localization of the heart rhythm determinants: connexin43, plakophilin-2, N-cadherin and plakoglobin during the female estrogen cycle. Use of these animal models considerably enriched our understanding of the cardiovascular system pathophysiology.

Keywords: chagas disease; chamber transcriptomic specificity; hypoxia; low-salt diet; metabolic syndrome; sex dichotomy; post-ischemic heart failure; pulmonary hypertension

1. Introduction

Human cardiovascular system is composed of a tetra-chambered heart that pumps the blood alternatively through the interconnected pulmonary and systemic vasculature circuits under the command of the sinoatrial node acting like a pacemaker [1]. The cardiovascular system's organization and function were practically conserved in the animal kingdom during the evolution starting with crocodilians stage [2]. Therefore, one can explore its physiopathology on vertebrate models, free of the legal, moral and religious constraints limiting experiments on living humans. Although the investigator has to follow the protocol approved by the local Institutional Animal Care and Use Committee (IACUC), animal models allow studies never permitted on living humans. IACUC's protocols should adhere to internationally recognized ethical principles [3] and respect the Guide for the Care and Use of Laboratory Animals [4].

In addition to species [5,6], the characteristics of the animal model depends on strain [7], sex [8], age [9], hormonal status [10], diet [11], housing [12], medical history (disease stage and applied treatments) [13], stress [14], and external stimuli [15] to name just a few. This review presents what we have learned from investigating the cardiovascular systems of mouse, rat and dog models.

 doi:10.20944/preprints202605.0124.v1

2. Materials and Methods

2.1. Transcriptome Analyses

2.1.1. Platform Used, Filtering and Normalization of Gene Expression Data

We carried out the genomic studies on Duke [16], Einstein [17], Rockefeller, and Yale [18] university microarray facilities, as well as on Agilent microarrays [19], using inhouse improved wet protocols and original mathematical algorithms and computer software. In order to choose the right platform, we quantified also the technical noise of Affimetrix microarrays, Illumina expression BeadChips and Illumina next generation MiSeq and NextSeq 550 RNA-sequencing by profiling technical replicates. Raw data and experimental protocols were deposited on the publicly accessible Gene Expression Omnibus of the (U.S.A.) National Center of Biotechnology Information within the National Library of Medicine.

Any spot with saturated or corrupted pixels, or with fluorescence foreground less than twice the background in one microarray was eliminated from the analysis in all microarrays hybridized in that experiment. Background subtracted fluorescence signal of every valid spot in a microarray was normalized the median of net signals of all valid spots of that microarray. When the slide was printed with several pins (like AECOM microarrays), the normalization was carried out separately for each pin-domain to minimize the errors of dropping slightly different amounts of cDNA.

2.1.2. Transcriptomic Characterization of Individual Genes

Gene expression data from four biological replicas of a particular tissue region in a given condition were fully exploited to characterize the individual genes by three independent measures: *AVE* = average normalized expression level across biological replicas, *REC* = relative expression control and *COR* = expression correlation with each other gene.

$$\forall gene\ i\ \&\ \forall condition/tissue\ c\ \rightarrow REC_i^{(c)} \equiv log_2\left(\frac{\langle REV^{(c)}\rangle}{REV_i^{(c)}}\right) \quad (1)$$

$where: RCS_i^{(c)} \equiv \frac{\langle REV^{(c)}\rangle}{REV_i^{(c)}}$ is the relative control strength (1a)

$\langle REV^{(c)}\rangle$ is the median $REV = chi - square\ midinterval\ of\ the\ coefficient\ of\ variation$

$$REV_i^{(c)} \equiv \frac{\sigma_i^{(c)}}{2AVE_i^{(c)}}\left(\sqrt{\frac{r_i}{\chi^2(\beta;r_i)}} - \sqrt{\frac{r_i}{\chi^2(1-\beta;r_i)}}\right) \quad (1b)$$

Positive *REC's* indicate stronger expression control while negative values indicate looser control with respect to that of the control of median gene in the profiled region. We consider genes critical for the cell phenotype expression, survival, and proliferation to be subjected to a stricter control of their expression levels, while those used for adapting the environmental changes are allowed to fluctuate.

COR is the pair-wise Pearson correlation coefficient of the (log_2) of the normalized

expression levels of the genes *i* and *j* in tissue/condition. We proved recently [20] that the set of all COR coefficients is a reasonable approximation of the transcriptome configuration function. We used also *COORD* = percentage of ($p < 0.05$) statistically synergistically expressed gene pairs plus percentage of antagonistically expressed pairs minus percentage of independently expressed genes within the analyzed pathways. Together, the percentage of synergistically expressed gene pairs and the percentage of antagonistically expressed pairs indicate how much coupled (i.e., influencing each-other's expression)-the genes are in the functional pathway.

The three independent features of individual gene expression are complemented with the derived characteristic *GCH*—gene commanding height:

$$\forall i\ \&\ \forall c\ \rightarrow\ GCH_i^{(c)} \equiv exp\left(REC_i^{(c)} + \langle\left(2COR_{i,j}^{(c)}\right)^2\rangle_j\right) \quad (2)$$

GCH is used to hierarchize genes according to their expression control and coordination with expression with other genes. We assumed and verified [21] that manipulation of genes with higher

 doi:10.20944/preprints202605.0124.v1

GCH has larger consequences on the transcriptome, the top gene, named Gene Master Regulator (GMR) being the most influential, so that its silencing might be lethal for the cell.

2.1.3. Genomic Fabric Landscape Through Full Characterization of Gene-Pairs

We defined the Pair-Wise Relevance (PWR) score that incorporates the entire expression information about the paired genes to construct the genomic fabric landscapes of individual functional pathways and of their interplay:

$$PWR_{i,j}^{(c)} \equiv \frac{\langle REV^{(c)} \rangle}{\langle AVE^{(c)} \rangle} \left| COR_{i,j}^{(c)} \right| \sqrt{\frac{AVE_i^{(c)} AVE_j^{(c)}}{REV_i^{(c)} REV_j^{(c)}}} \quad (3)$$

2.1.4. Expression Regulation of Individual

Expression of a gene is considered significantly regulated in a particular cardiovascular condition or tissue location with respect to the healthy counterpart or another tissue location it satisfies the composite criterion of the absolute fold-change "x" exceeding the cut-off "CUT" and the p-value is less than 0.05 p-value of the heteroscedastic t- test of means' equality. "CUT" is computed for each gene and encompasses both the technical noise of the gene expression technology and the biological variability:

$$\begin{cases} \left| x_i^{(disease\ vs\ normal)} \right| > CUT_i^{(disease\ vs\ normal)} \\ p_i^{(disease\ vs\ normal)} < 0.05 \end{cases} \quad (4)$$

$$\text{Where: } x_i^{(disease\ vs\ normal)} = \begin{cases} \frac{AVE_i^{(disease)}}{AVE_i^{(normal)}}, if\ AVE_i^{(disease)} > AVE_i^{(normal)} \\ -\frac{AVE_i^{(normal)}}{AVE_i^{(disease)}}, if\ AVE_i^{(disease)} \leq AVE_i^{(normal)} \end{cases} \quad (4a)$$

$$CUT_i^{(disease\ vs\ normal)} = 1 + \sqrt{\frac{2}{100}\left(\left(REV_i^{(disease)} \right)^2 + \left(REV_i^{(normal)} \right)^2 \right)} \quad (4b)$$

Expression regulation of certain critical genes was "validated" through two-step quantitative real-time polymerase chain reaction (qRT-PCR) SYBR Green method (Applied Biosystems) as described in [22]. However, given the technical noises of both microarray and qRT-PCR, confirmation of small expression ratios was doubtful. In parallel, we used also Western Blotting and immunolabeling and epifluorescence microscopy to determine abundances of several critical proteins and their subcellular localization. Nevertheless, validation of the regulation of a few of the genes identified by a high throughput method has no statistical relevance.

2.1.5. Regulation and Remodeling of Individual Genes and Functional Pathways

Our analyses were focused on the genes selected by KEGG (Kyoto Encyclopedia of Genes and Genomes as included in several specialized functional pathways) [23]. The functional pathways were globally characterized by median REC of the individual genes and the network of the ($p < 0.05$) significantly synergistically and antagonistically expressed genes.

Alterations of gene expression profiles are usually quantified by the percentages of significantly up- and down-regulated genes that implicitly consider each affected gene as an equal +1 or −1 contributor. Therefore, for a comprehensive characterization of the transcriptomic alteration of a functional pathways "Γ" to the expression difference between the compared phenotypes, we introduced the Weighted Individual (Gene) Regulation (WIR) and the Weighted Pathway Regulation (WPR):

$$WIR_i^{(disease\ vs\ normal)} \equiv AVE_i^{(normal)} \left(\left| x_i^{(disease\ vs\ normal} \right| - 1 \right) \left(1 - p_i^{(disease\ vs\ normal} \right) \quad (5)$$

$$WPR_{(\Gamma)}^{(disease\ vs\ normal} = \frac{1}{Card(\Gamma)} \sqrt{\sum_{i \in \Gamma} \left(WIR_i^{(disease\ vs\ normal)} \right)^2} \quad (6)$$

WIR takes into account the absolute change of the expression level and the statistical confidence of the expression alteration of an individual gene, while *WPR* extends this measure to all pathway genes.

 doi:10.20944/preprints202605.0124.v1

The transcriptomic distance $TD^{(c2\ vs\ c1)}$ between two conditions *c1* and *c2* is defined as the Euclidian distance separating condition *c2* from the origin (*c1*) of the 3D dimensional space (*AVE, REC, COR*) where each axis is normalized to the respective median in *c1*:

$$TD_{\Gamma}^{(c2\to c2)} \equiv \sqrt{\frac{1}{N}\left(\sum_{i\in\Gamma}\left(\frac{\left(AVE_i^{(c2)}-AVE_i^{(c1)}\right)}{\langle AVE^{(c1)}\rangle}\right)^2+\left(\frac{\left(REC_i^{(c2)}-REC_i^{(c1)}\right)}{\langle REC^{(c1)}\rangle}\right)^2+\sum_{j\in J}\left(\frac{\left(COR_i^{(c2)}-COR_i^{(c1)}\right)}{\langle COR^{(c1)}\rangle}\right)^2\right)} \quad (7)$$

2.1.6. Transcriptomic Recovery

Transcriptomic alterations of a functional pathway "Γ" associated to a cardiovascular disease can be totally or partially recovered with respect to the normal state "Π" by an adequate treatment, "Θ". We quantified the transcriptomic effect of treatment with respect to not treated disease "Ω" by two measures, TRE = transcriptomic recovery efficiency and PRE = pathway restoration efficiency. TRE relies on the percentages of significantly regulated genes in diseased untreated and diseased treated subjects.

$$TRE_{(\Gamma)}^{(\Theta)} = \frac{D_{(\Gamma)}^{(\Omega)}X_{(\Gamma)}^{(\Theta)}+U_{(\Gamma)}^{(\Omega)}X_{(\Gamma)}^{(\Theta)}-X_{(\Gamma)}^{(\Omega)}D_{(\Gamma)}^{(\Theta)}-X_{(\Gamma)}^{(\Omega)}U_{(\Gamma)}^{(\Theta)}}{D_{(\Gamma)}^{(\Omega)}X_{(\Gamma)}^{(\Theta)}+U_{(\Gamma)}^{(\Omega)}X_{(\Gamma)}^{(\Theta)}+X_{(\Gamma)}^{(\Omega)}D_{(\Gamma)}^{(\Theta)}+X_{(\Gamma)}^{(\Omega)}U_{(\Gamma)}^{(\Theta)}+D_{(\Gamma)}^{(\Omega)}D_{(\Gamma)}^{(\Theta)}+U_{(\Gamma)}^{(\Omega)}U_{(\Gamma)}^{(\Theta)}+D_{(\Gamma)}^{(\Omega)}U_{(\Gamma)}^{(\Theta)}+U_{(\Gamma)}^{(\Omega)}D_{(\Gamma)}^{(\Theta)}}\times 100\% \quad (8)$$

$$where: D, U, X = percentage\ of\ significant\ down-, up-, no\ regulation$$

There are four possible outcomes:

$$\begin{cases} TRE_{(\Gamma)}^{(\Theta)} = 100\% & \to \quad ideal\ (no\ regulated\ genes\ after\ treatment) \\ 0 \le TRE_{(\Gamma)}^{(\Theta)} \le 100\% & \to \quad posutive\ (fewer\ regulated\ gene\ after\ treatment \\ TRE_{(\Gamma)}^{(\Theta)} = 0\% & \to \quad null\ (unchanged\ number\ of\ regulated\ genes) \\ TRE_{(\Gamma)}^{(\Theta)} < 0\% & \to \quad negative\ (more\ regulated\ genes\ after\ treatment \end{cases} \quad (9)$$

$$PRE_{(\Gamma)}^{(\Theta)} = \left(1-\frac{WPR_{(\Gamma)}^{(\Theta\ vs\ \Pi)}}{WPR_{(\Gamma)}^{(\Omega\ vs\ \Pi)}}\right)\times 100\% \quad (10)$$

There are four possible outcomes:

$$\begin{cases} WPR_{(\Gamma)}^{(\Theta\ vs\ \Pi)} = 0 & \to \quad PRE_{(\Gamma)}^{(\Theta)} = 100\% \quad recovered \\ 0 < WPR_{(\Gamma)}^{(\Theta\ vs\ \Pi)} < WPR_{(\Gamma)}^{(\Omega\ vs\ \Pi)} & \to \quad 0 < PRE_{(\Gamma)}^{(\Theta)} < 100\% \quad improved \\ WPR_{(\Gamma)}^{(\Theta\ vs\ \Pi)} = WPR_{(\Gamma)}^{(\Omega\ vs\ \Pi)} & \to \quad PRE_{(\Gamma)}^{(\Theta)} = 0\% \quad null \\ WPR_{(\Gamma)}^{(\Theta\ vs\ \Pi)} > WPR_{(\Gamma)}^{(\Omega\ vs\ \Pi)} & \to \quad PRE_{(\Gamma)}^{(\Theta)} < 0\% \quad worse \end{cases} \quad (11)$$

By evidence, *PRE* is a more realistic transcriptomic evaluation of treatment efficiency in restoring the normal gene expression profile.

2.2. Physiology Studies

2.2.1. Analyses

On a dog model of the metabolic syndrome, we performed echocardiography with an Acusan 356 Sequoia in both longitudinal and M-mode views [24] to determine the heart rate, stroke volume and left ventricle systole and diastole diameter. In addition, cardiac output, fractional shortening, coronary vascular resistance and total peripheral resistance were also measured. Hemodynamic investigations included measurement of coronary blood flow with a Doppler flow transducer, of systolic, diastolic, mean arterial and end-diastolic blood pressure with a recording pressure transducer, and of the left ventricle pressure rise with an operational amplifier. Blood samples were used to determine the concentrations of glucose, plasma insulin, angiotensin II, uric acid, homocysteine, and both high- and low-density lipids.

2.2.2. Data Transformation and Pathology Quantification

One of the most difficult tasks of the medical doctor is to make sense of the wide diversity of the parameters to consider when establishing the diagnostic and decide about the therapeutic approach. What is worst, a blood sugar (GLU) of 129 mg/dL (reference range 65–99 mg/dL), 1.97 mg/dL

 doi:10.20944/preprints202605.0124.v1

creatinine CRE, (reference 0.70–1.28 mg/dL), or 0.3 mlU/L thyroid stimulating hormone (TSH, reference range 0.4–4.5 mlU/L)? Since it is practically impossible to correct everything at once and almost all treatments have side effects, it is very important to decide what altered characteristic(s) should be corrected first. Therefore, we used to transform the concrete parameters into non-dimensional pure numbers using their considered physiological intervals that can be compared and integrated into a mathematical model.

$$z_i = \frac{a_i - \mu_i}{\sigma_i}, where: z_i \epsilon (-1, +1)\ is\ the\ dimensionless\ physiological\ interval, \quad (12)$$

$$\left(a_i^{(\min)}, a_i^{(\max)}\right)\ is\ the\ real\ physiological\ interval, \quad (12a)$$

$$\mu_i \equiv \frac{a_i^{(\min)} + a_i^{(\max)}}{2}, \sigma_i \equiv \frac{a_i^{(\max)} - a_i^{(\min)}}{4} \quad (12b)$$

Thus, the dimensionless measures of the above values become: GLU = 5.53, CRE = 6.76, TSH = -2.10, indicating for this set that creatinine alteration is the worst of the three and should be carried out first.

The dimensionless z-scores were used to build a multi-dimensional pre-Hilbert space of physiological and pathological states. This space has as many dimensions as many independent parameters are considered. Then one may compute the so-called "patholog" $\boldsymbol{P}$ of the disease $\boldsymbol{D}$ as the normalized Euclidian distance between the point representing the actual state and the unit, 0-centered hypersphere representing the subspace of stable physiological states. Change of patholog due to progression of the disease or in response to a treatment is quantified by the score "F" [25].

$$P(disease) = \begin{cases} \frac{1}{N}\sqrt{\sum_i \left(z_i^{(disease)}\right)^2} - 1 & if \quad \sum_i \left(z_i^{(disease)}\right)^2 > 1 \\ 0 & if \quad \sum_i \left(z_i^{(disease)}\right)^2 \leq 1 \end{cases} \quad (13)$$

$$F\left(_{result}^{(treatment)}\right) \equiv \left(1 - \frac{P_{(final)}^{(disease)}}{P_{(initial)}^{(disease)}}\right) \times 100\% \quad (14)$$

There are four interesting cases:

$$\begin{cases} P_{(final)}^{(disease)} = 0 & \rightarrow & F\left(_{result}^{(treatment)}\right) = 100\% & cured \\ 0 < P_{(final)}^{(disease)} < P_{(initial)}^{(disease)} & \rightarrow & 0 < F\left(_{result}^{(treatment)}\right) < 100\% & improved \\ P_{(final)}^{(disease)} = P_{(initial)}^{(disease)} & \rightarrow & F\left(_{result}^{(treatment)}\right) = 0\% & null \\ P_{(final)}^{(disease)} & \rightarrow & F\left(_{result}^{(treatment)}\right) < 0\% & worse \end{cases} \quad (15)$$

2.3. Histology and Apoptosis Detection

Surgically removed hearts were immersed overnight in 4% paraformaldehyde and then transferred to 75% ethanol before being stained with hematoxylin-eosin and embedded in paraffin. Cardiomyocyte transversal area was evaluated using image AxioVision 4.1 software (Zeiss, Thornwood, NY).

We used TUNEL assay (Roche Applied Science) to identify and counted with AxioVision 4.1 at fluorescence microscope the apoptotic nuclei stained with DAPI in deparaffinized and rehydrated heart sections.

3. Results

3.1. Sex is an Important Transcriptomic Regulator

Duke mouse microarrays [16] were used to profile separately the gene expressions in the ventricles and atria of four adult C57Bl/6j male and their sibling females (in diestrus) mice], experimental protocol (approved by AECOM IACUC and raw data publicly available in the Gene Expression Omnibus of the National Center for Biotechnology Information (NCBI/GEO) [26]. We quantified the expression levels, control and correlation of 66 selected heart rhythm determinant

 doi:10.20944/preprints202605.0124.v1

(HRD) genes [27] and found that they have on average larger expression in male than in female atria, but lower average expression in male than in female ventricles.

This study has shown for the first time the substantial sex differences in the HRD expression control of individual genes [27], although the averages were practically the same for the two sexes in both atria and ventricles. For instance, the expression control of *Atp1a2* (ATPase Na+/K+ Transporting Subunit Alpha 2), encoding a sodium-potassium pump that protects against beta-adrenergic desensitization in myocardial infarction [28], is in the 98th percentile in female atria but only in the 11th percentile in males. However, control of *Gja5* (encoding connexin 40, the main gap junction protein interconnecting the atrial cardiomyocytes [29]) and that of *Gja1* (encoding connexin 43, the main gap junction protein linking the ventricle cardiomyocytes [30]) were practically the same for both sexes. The ($p < 0.05$) statistically significant networking (measured by the sum of the percentages of synergistically and antagonistically expressed pairs) of HRD genes was stronger in female than in male atria, while the networking was stronger in male than female ventricles. These results may partially explain why the PR interval is longer in men, while women have higher resting heart rate and longer QT interval [31,32], as well as the implications of the female estrous cycle [33].

3.2. Heart Transcriptome Topology Changes During Development

We profiled the gene expressions in the ventricles of CD1 mice of 1, 2 and 4 weeks of age with 27k cDNA microarrays printed by AECOM Microarray facility [17]. It was part of a complex study of developing mice under normal atmospheric conditions or to chronic intermittent or constant hypoxia [22] funded by a 10y NIH PPG with protocols approved by AECOM and Yale University IACUCs. Looking to the expression data [34], we found over 40% (sic!) of the genes as significantly up or down-regulated between the two successive developmental stages. Interestingly, some genes kept the same tendency in the second interval, while other being oppositely regulated. For instance, *Stard10* (START domain containing 10) was up-regulated in both intervals ($x^{(2w \text{ vs } 1w)} = 3.78$, $x^{(4w \text{ vs } 2w)} = 2.42$) and *Shkbp1* (Sh3kbp1 binding protein 1) was down-regulated in both intervals ($x^{(2w \text{ vs } 1w)} = -10.33$, $x^{(4w \text{ vs } 2w)} = -2.40$). For other genes, regulation in first interval was corrected in the second. Thus, the up regulation of *Pdcd8* (Programmed cell death 8) in the first interval was fully corrected in the second ($x^{(2w \text{ vs } 1w)} = 4.60$, $x^{(4w \text{ vs } 2w)} = -4.97$, resulting $x^{(4w \text{ vs } 1w)} = -1.08$). By contrast, the downregulation of *Disp1* (Dispatched homolog 1) was corrected in the second ($x^{(2w \text{ vs } 1w)} = -38.45$, $x^{(4w \text{ vs } 2w)} = 27.71$, resulting $x^{(4w \text{ vs } 1w)} = -1.39$).

3.3. Each Heart Chamber Has a Distinct Transcriptomic Topology

Agilent 4x44K Whole Mouse Genome Microarrays [35] were used to profile separately the gene expressions in the myocardial wall of each atrium and ventricle from hearts of 4 adult C57bl/j male mice (AECOM IACUC approved protocol and raw data in [36,37]). The purpose of this study [38] was to determine whether there is any transcriptomic basis for the distinct function of each chamber [39–41]. Interestingly, out of 16,886 quantified unigenes in every chamber, 2661 (i.e., 15.76%) were differently expressed between the left atrium and the left ventricle, 2786 (16.50%) between the right atrium and the right ventricle, while 979 (5.8%) between the two atria and only 202 (1.2%) between the two ventricles. The large differences between the atrium and ventricle from each side, and the much smaller between the two ventricles can be explained how the mouse heart developed from mesodermal cells starting with E7.5 with the formation of the heart tube. The heart tube splits initially into an atrium and a ventricle, then the atrium subdivides into the left and the right atria, followed at the last stage by the splitting the ventricle into the left and the right ventricles [42]. We have shown for the first time that the transcriptomic distinction among the heart chambers extends to the expression control and networking of genes encoding membrane ion channels and transporters. Moreover, [38] results indicate that each chamber has its own transcriptomic topologies of the adrenergic signaling in cardiomyocytes [43], calcium signaling [44], cardiac muscle contraction [45], glycolysis/gluconeogenesis [46], and oxidative phosphorylation pathways [47].

 doi:10.20944/preprints202605.0124.v1

3.4. Expression Level and Subcellular Localization of Intercalated Disk Proteins Changes During Estrogen Cycle in Female Heart

An in-house improved procedure and quantification of Western blotting [48] was used to determine the abundances of selected cardiomyocyte intercalated disk proteins in atria and ventricles of 8 weeks old 12 C57Bl/6j mice. The experimental protocol was approved by AECOM IACUC. The mice were split in three groups of 4: Gr.1: males, Gr.2: females in estrus and Gr.3: females in diestrus. The phase of the estrus cycle was determined daily by vaginal lavage and cytology examination at microscope [49]. Subcellular localizations of connexin43, plakophilin-2, N-cadherin and plakoglobin, ankyrin-2 and actin were determined using methods inspired from the Musil and Goodenough protocol to separate the level of connexin43 in membrane and cytosol by differential solubilization in Triton X-100 [50]. We concluded that not only the gene expression profiles, control and networking are different between the two sexes but even the subcellular localization of several proteins involved in mechanical and electrical coupling of the cardiomyocytes change during the female estrous cycle [48]. Therefore, one needs to consider also the sex hormonal status in studies on female animal models [51,52].

3.5. Transcriptomic Consequences of Low Salt Diet

We have proved that the benefic effects of law-salt diet [53] partially result from the remodeling of the transcriptomic topology of metabolic and signaling functional pathways. For this, we profiled the gene expression in the left ventricles of 16 adult C57Bl/6j male mice fed for the last 8 weeks with regular (0.4% Na) or law-salt (0.05% Na) diet [54]. Experimental studies (protocol approved by NYMC IACUC) has shown that the law-salt diet increased the expression control of fatty-acids biosynthesis [55] but decreased that of steroid hormones [56]. We noted also [57] that the law-salt diet had substantial effects on the transcriptomic topology of functional pathways responsible for Chagas disease [58] and diabetic [59], dilated [60] and hypertrophic [61] cardiomyopathies. It has significantly reduced the transcriptomic correlation between glycolysis/gluconeogenesis [46] and cardiac muscle contraction [45] pathways, as well as that between hypertrophic cardiomyopathy pathway with cardiac muscle contraction [45] pathway through the adrenergic signaling [43] pathway. In terms of Weighted Pathway Regulation (WPR, eq. 6), the most affected pathways were: Cardiac Muscle Contraction (WPR = 45.30 for 75 quantified unigenes) and Oxidative Phosphorylation (WPR = 37.42, 110 genes), substantially larger than the WPR = 15.67 for all 19,605 properly quantified unigenes.

3.5. Transcriptomic, Morphological and Physio Pathological Consequences of Chronic Constant Hypoxia (CCH)

We used a mouse model to determine the genomic mechanisms that may be responsible for the effects of chronic constant hypoxia (CCH) [22,62] as it happens in pulmonary disease or living at high altitude (> 2500 m) on heart morphology and physiology [63]. For this purpose, we compared the heart results of CD1 mice housed in Biospherix chambers starting postnatal day 2 for 1, 2 or 4 weeks, where oxygen concentration was constantly maintained at 11% with their sibling housed at normal atmospheric conditions (oxygen concentration 21%). Experimental protocols were approved by AECOM and Yale University IACUCs. Gene expressions were profiled with AECOM 27k mouse oligodendrocyte microarrays [17], gene expression data in [34]). Our CCH study revealed significantly slower development (less than normal increase of bodyweight), but substantial heart enlargement (especially of the right ventricle), more total protein content and higher hematocrit. Hypoxia induced substantial alterations of the expression level, control and inter-coordination of numerous genes and remodeled several major functional pathways. Genes such are: *Ccnb1, Eif3s2, Eif4ebp2, Fhl1, Hif1a, Miki67, Pcna, Tbx5,* and *Tro* exhibited significant changes of the maturation profile compared to the corresponding normoxic profiles [62]. We found also upregulation of both gene expression and protein levels of the eukaryotic translation initiation factors *Eif2a* and *Eif4e*. The observed enhanced apoptosis was in relation with the upregulation of pro-apoptotic genes and

 doi:10.20944/preprints202605.0124.v1

downregulation of anti-apoptotic ones. Overall, the coordination degree was reduced from 20% to 8%. However, the significant expression intercorrelations of *Hif1a* (hypoxia-inducible factor 1-alpha, [64]) and 32 genes involved in the heat shock response [65] increased from 7% synergistic and 7% antagonistic to 35% synergistic and 12% antagonistic justifying the roles of these genes in the vascular development [64].

3.6. Transcriptomic, Morphological and Physio Pathological Consequences of Chronic Intermittent Hypoxia (CIH)

Snoring and sleep apnea are recognized causes of cardiovascular diseases [66–68]. Such conditions were mimicked by housing CD1 mice in Biospherix chambers starting postnatal day 2 for 1, 2 or 4 weeks, where oxygen concentration was switched every 4 min between 11% and the normal 21% (intermittent hypoxia) [22,69]. Transcriptomic consequences of this intermittent oxygen deprivation were severe, yet significantly different than those of constant hypoxia. A notable difference was the downregulation of *Eif4e* (eukaryotic translation initiation factor 4E), an oxygen-regulated switch in protein synthesis [70], in contrast with its up regulation in constant hypoxia suggesting the role of the encoded protein in cardiac hypertrophy. The maturational profiles of *Ccnb1, Eif3s2, Eif4ebp2, Fhl1, Hif1a, Miki67, Pcna, Tbx5,* and *Tro* were again altered, yet differently of what was found in constant hypoxia. In [71] we reported the regulation of the expression of heart rhythm determinant genes, significant decoupling of their inter-coordination and remodeling of the Ca^{+2} [72] and Wnt [73] signaling pathways. Importantly, the transcriptomic alterations in hypoxia exposed mice with respect to the normoxic ones decreased from the first week to the fourth, suggesting a kind of adaptation to the oscillating atmospheric conditions.

4. Animal Models

4.1. Chagas Disease

Chronic Chagas Cardiomyopathy (CCC), affecting people in Latin America for more than 9,000 years, was first described in 1909 by the Brazilian doctor Carlos Chagas. CCC is observed in 10 to 30% of individuals infected with the hemoflagellated protozoan parasite *Trypanosoma cruzi* [74] leads to cardiomegaly associated with arrhythmias and congestive heart failure (CHF), resulting in over 10,000 worldwide annual deaths [75]. The disease is endemic in the entire Latin America but evolved into a global disease due to international travel and migration of infected individuals. CCC is characterized by inflammatory infiltration with myonecrosis and myocytolysis, intense interstitial fibrosis, apical ventricular aneurysm], and arrhythmia [76–78]. Remodeling of the myocardium and vasculature is the result of damage to the extracellular matrix and the replacement of myocytes and/or vascular cells by fibrous tissue leading to myocardium thinning and hypertrophy of the remaining cardiac myocytes. [77]

4.1.1. Experimental Methods

For over two decades, IacobasLab was involved in collaborative research with Chagas Institute from Rio de Janeiro (Brazil) on mouse ([79]) and rat [80] (expression data in [81]) models of Chagas disease, both at the level of ventricular walls [82] (expression data in [83]) as at isolated cardiomyocytes [84] (expression data in [85]). We have also compared the transcriptomic effects of cardiomyocyte infection with four major strains of *Trypanosoma cruzi* [80]*:* Brazil, CL (Colombian) Brener, Tulahuen, and Y [86–88], identifying Tulahuen strain as the most disruptive from the four [80].

The entire animal work was performed at Chagas Institute from Rio de Janeiro, Brazil, whose IACUC approved the experiments. Left ventricular function was routinely evaluated using echocardiography and cardiac electrophysiology. Right ventricular dilatation, an important index of the severity of Chagas disease in infected mice, was measured with cardiac gated MRI as chamber

 doi:10.20944/preprints202605.0124.v1

diameter and volume in both systole and diastole. Delayed gadolinium enhancement MRI was used to identify fibrosis regions in vivo. Multimodality microPET/microCT with a contrast agent (Exitron Nano 12000, Viscover) was used for contrast between the ventricular blood and myocardium. With 18F-FDG our collaborators observed alterations in heart glucose uptake before structural or functional changes were detected by MRI or echocardiography [89–91].

4.1.2. Parasite Infection and Development of Chagas Disease

Chagas disease was induced in C57Bl/6j, BALB/c and 129 mouse strains through intraperitoneal injection of ~10^4 CL, Brazil or Tulauen trypomastigotes, in many cases collected from cultures of infected Rhesus Macaca Mulatta LCC-MK2 cells [92]. The studies revealed alterations of major functional pathways including the immune response, JAK/STAT signaling and cell cycle pathways [93–95]. We explained the observed impairment of the synchronous heat contractions by the downregulation of the gene *Gja1* (Gap Junction Protein Alpha 1, [96]) and the abundance of connexin 43 that it encodes [97]. We [98] and other groups [99–102] proved the mitochondrial collapse as one major factor of the Chagas cardiomyopathy.

Figure 1 presents the PWR (computed with equation 3) landscape of the HRD and Immune Inflammatory Response (IIR) genomic fabrics and their interplay in the left ventricle of control and infected mice. Of note is leveled HRD fabric in infected mice, meaning reduced heart rhythm determinant activity, while the IIR fabric exhibits substantial increase of peak values, indicating elevated immune response through inflammatory cytokines like interferons and tumor necrosis. It is also interesting to observe changes in the PWRs of HRD-IIR pairs in the infected mice, suggesting alteration of the interaction of the two fabrics.

4.1.3. Cell Therapy for Chagas Disease

What is the most effective, yet affordable, therapeutic response too CCC is still under debate. Administration of specific anti-parasitic drugs to humans in the acute phase clears the peripheral blood of parasites but does not stop the progression to CCC [103]. There have been numerous attempts to develop anti-*T. cruzi* vaccines (e.g., cruzipain [104], Traspain [105]), but none so far proved reliable enough to be included in clinical trials [106]. For individuals with CCC and CHF, heart transplantation is often the only therapeutic option. However, heart transplantation is expensive and associated with a variety of problems including reactivation of the infection [107]. As alternative therapy, we [108] and other groups [109] have tested stem cell-based treatment in experimental mouse [110] and dog models [111].

Bone marrow cells (BMCs), known to normally migrating to the inflamed heart once released in the blood [112], were collected from femurs and tibias of 6 weeks old BALB/c, C57BL/6 EGFP, or B6.129 Gtrosa26 mice to be administrated to Chagasic mice [113,114]. Mesenchymal mononuclear cells (MSC) were obtained by purifying 15 min centrifugation at 1000g in Ficoll gradient then washed, filtered and resuspended in saline. 3x10^6 MSCs were injected intravenously in each Chagasic mice six months after parasitic infection. Blood circulation drives the stem cells to the heart. The treatment substantially reduced the right ventricular enlargement [110], and the abundances of the inflammatory infiltrates (quantified by the galectin-3 level, [108]) and the interstitial fibrosis [114].

 doi:10.20944/preprints202605.0124.v1

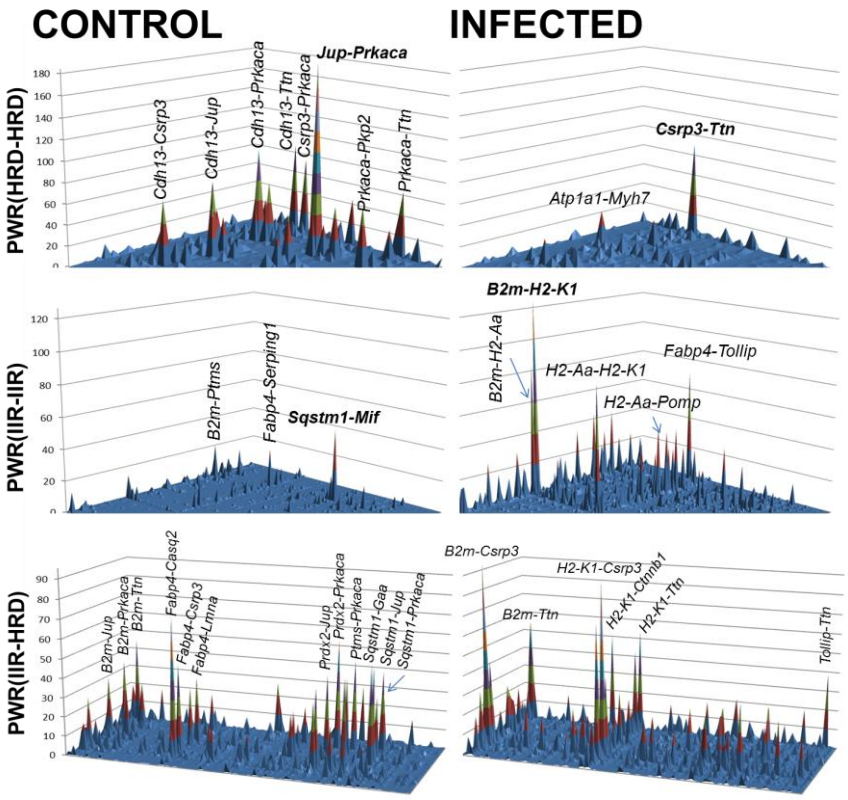

Figure 1. PWR landscape of the Heart Rhythm Determinant (HRD) and Immune-Inflammatory Response (IIR) genomic fabrics and their interplay in control and infected mice, indicating also the most prominent gene-pairs. Note that infected mice have reduced transcriptomic roles of heart rhythm determinant (HRD) genes but substantial increase of the inflammatory-immune response (IIR) ones together with the remodeling of the transcriptomic interplay of the two genomic fabrics. Important genes: *B2m* (beta-2 microglobulin), *Casq2* (calsequestrin 2), *Csrp3* (cysteine and glycine-rich protein 3), *Fabp4* (fatty acid binding protein 4, adipocyte), *H2-K1* (histocompatibility 2, K1, K region), *Jup* (junction plakoglobin), *Mif* (macrophage migration inhibitory factor), *Prkaca* (protein kinase cAMP-activated catalytic subunit alpha), *Sqstm1* (sequestosome 1), *Ttn* (titin).

Cell treatment recovered the normal expression of most of the affected genes even though it also altered expression of a few other genes (Figure 2) so that for the entire profiled transcriptome the two scores were: TRE = 84% [108] and PRE = 72% [115].

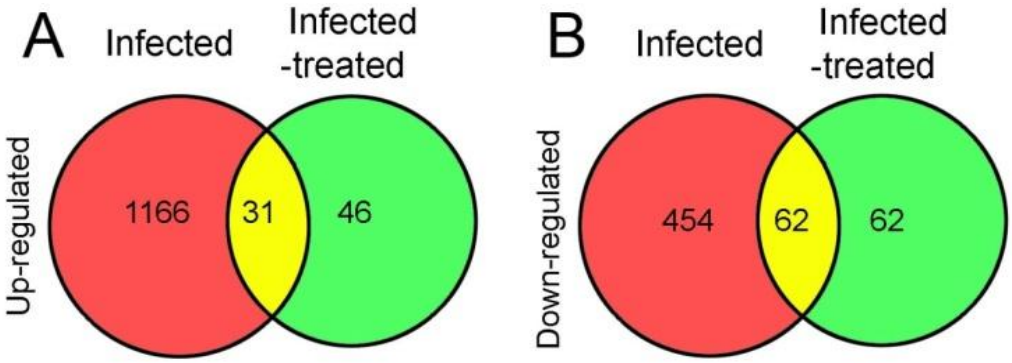

Figure 2. Venn diagrams indicating recovery of gene expression in response to cell treatment of mouse *Trypanosoma cruzi* infected heart. In infected heart, 1197 genes were found as upregulated, and all but 31 were restored to normal level, while other 46 genes were upregulated by the treatment. In addition, 516 genes were

 doi:10.20944/preprints202605.0124.v1

downregulated by infection, 390 of which were restored to normal levels, while 62 additional genes were downregulated by the treatment. .

Moreover, the treatment adjusted the expression control and remodeled the gene networks of several functional pathways, including the cardiac muscle contraction [45], chemokine signaling [116], Chagas disease [58] and mitochondrial respiratory chain [47].

4.2. Post-Ischemic Heart Failure

Ischemic cardiomyopathy, a major cause of death worldwide (~800,000 patients in U.S.A. alone), occurring when heart blood supply is reduced below critical levels by partial occlusion of coronary arteries, leads to myocyte loss from the heart walls [117]. Myocardial necrosis is responsible for increased systolic and diastolic stress and heart rate, ventricular hypertrophy until rupture and aneurism [118]. Infarction scar generates a strong inflammatory response through accumulation of polynuclear leukocytes and release of cytokines [119]. Ischemic cardiomyopathy is usually assessed through computer tomography of the myocardial perfusion [120].

Our studies on a mouse model of post-ischemic heart failure (developed by our collaborators from Universidade Federal do Rio de Janeiro with local IACUC approval) revealed substantial increases of total serum immunoglobulin M (by 5.2x) and G (by 3.6x), circulating cytokines (IFN-γ by 3.1x, IL-1β by 3.8x, IL-8 by 13.0x and TNF-α by 6.0x,) [121]. Myocardial infarction has direct impact on all other organism systems, including substantial increase of the depression prevalence [122], with Chemokine (C-X-C motif) ligand 12 (CXCL12) and Chemokine (C-C motif) ligand 2 (CCL22) potentially responsible for inducing depression after post-ischemic heart failure [123].

4.2.1. Induction of Ischemic Heart Failure in a Mouse Model

Anesthetized by ketamine (40 mg/Kg) intraperitoneal injection and intubated with a 100 cycles/min ventilator, 8w-old male and female C57Bl/6 had ligated the descending branch of the left coronary at 1mm from the left atrium tip. Control mice were subjected to the same surgical procedure excepting coronary ligating [121]. Ventricle myocardia were collected from all sham operated, infarcted not treated and cell treated mice and the gene expressions were profiled using AECOM 32k mouse oligonucleotide microarrays [17]. 3-lead electrocardiogram was continuously recorded starting 24 h post-surgery and heart rate, P, QRT, T wave amplitude and the PR, QRS and QT intervals were analyzed. Blood was collected from the caudal vein before and 3 days post-surgery, and several serum markers including cardiac troponin and creatinine kinase were dosed. In addition, heart contractions were imaged with a GE vivid 7 Megas color echocardiograph. The animal work was carried out at Universidad Federal do Rio de Janeiro with the approval of the local IACUC and the tissues were shipped to AECOM IacobasLab for transcriptomic profiling.

4.2.2. Heart Transcriptomic Changes in Infarcted Mice

Overall, the induced ischemia regulated 2158 (18%) of the 11981 unigenes properly quantified [121]. Microarray detected expression regulations of genes such are: *Hif1a, Ifnar1, Mmp23, Nos2* and *Tlr4* were qRT-PCR validated beyond the inherent technical noises of the two methods, with a Pearson pair-wise correlation coefficient of 0.968. The significantly up-regulated genes include chemokines (*Clc8, Ccl9, Cxcl14*), chemokine-like receptors (*Ifnar1, Ifngr1, Ifngr2*), interferon activated genes (*Ifi204, Ifi205, Isg20, Icsb1, Ifih1, Ifi1*), interleukins (*Il113, Il1f9*), interleukin receptors (*Il1r1, Il13ra1, Il2rg, Il22ra1*), interleukin-1 receptor-associated kinases (*Irak1, Irak2, Irak3, Irak4*), and tumor necrosis factor receptors (*Tnfrsf1a, Tnfrsf1b, Tnfrsf10b, Tnfrsf12a, Tnfrsf19l, Tnfrsf22, Tnfrsf25*). Importantly, no inflammatory/immune response gene was found to be significantly downregulated. Among others, we found that 22 out of 32 quantified genes from Complex 1 of the respiratory chain [47], 2/3 from Complex 2, 4/8 from Complex 3, 4/8 from Complex 4 and 4/6 were downregulated by ischemia. In addition, the inter-complexes expression coordination scores were substantially reduced from 16.25% in control to -2.50% for Cx1-Cx2, from 14.81% to 7.41% for Cx2-Cx3, from 16.67% to -

 doi:10.20944/preprints202605.0124.v1

1.19% for Cx3-Cx4, and from 13.57% to 2.14% for Cx4-Cx5. Positive COORDs indicate prevalence of significantly synergistically and antagonistically expression coordination, while negative values indicate that more genes were independently than coordinately expressed. Thus, cellular respiration was twice affected: first by reduced expression levels of the responsible genes and then by their diminished expression synchrony, important for the normal electron transfer between complexes [124]. These findings justify development of therapeutic strategies targeting mitochondria in cases of heart ischemic failure [125]. We reported also the infarct-triggered remodeling of *Adra1b* (alpha-1B adrenergic receptor (α1B-adrenoreceptor) expression correlation within the functional pathway Adrenergic signaling in cardiomyocytes [43], including switching the synergistic expression with *Crem* (CAMP-responsive element modulator) in healthy mice to antagonistic in infarcted animals [126].

4.2.3. Cell Therapy for Post Ischemic Heart Failure

We used the same cell therapy procedure for ischemic as for the Chagasic mice, excepting that stem cells were injected directly into the heart scar, and compared the results of saline treated with MSC treated infarcted animals. Treated animals exhibited better electrocardiograms (absence of the Q wave), systolic performance and oxygen consumption, and reduced ventricular dilatation. Administration of bone marrow derived mononuclear restored the normal expression of 2099 (96.2%) from the regulated genes in untreated animals, although 286 genes not affected by ischemia were regulated by cell treatment [127]. The treatment even reversed the upregulation of some genes. For instance, the expression ratio of *Ankrd1* (Ankyrin repeat domain 1, cardiac muscle, important cardiac repair [128]) switched from +2.09x in saline treated to -2.29x in cell treated with respect to healthy mice. Expression ratio of *Snx5* (Sorting nexin 5, critical for resisting cardiac failure through ventricle hypertrophy [129]) switched from +1.90x to -8.07x. The treatment restored partially the inter-complexes expression coordination to: 3.75% for Cx1-Cx2, 7.41% for Cx2-Cx3, 7.14% for Cx3-Cx4, and 6.43% for Cx4-Cx5.

4.3. Pulmonary Hypertension

The main features of the hemodynamic condition termed pulmonary hypertension (PH) are: mean pulmonary arterial pressure (mPAP) over 20 mmHg, pulmonary arterial wedge pressure (PAWP) less than 15 mmHg, and over 2 Wood Units pulmonary vascular resistance (PVR) [130]. PH comes from pathophysiology of both large and micro blood vessels. Stenosis of large vessels leads to intraluminal obstruction, vascular wall thickening and extrinsic compensation, while the morphological alteration of microvasculature translates into their occlusion, functional stenosis and pressure-backward transmission [130]. Clinically, PH development occurs in six stages: 1) hypertrophy of the arteriole middle layer, 2) intima thickening, 3) intimal fibrosis, 4) formation of plexiform lesions, 5) extensive fibrosis and hemosiderosis, 6) vascular necrosis [131,132].

4.3.1. Induction of Pulmonary Hypertension in Rat Models

Currently, one can study the molecular characteristics of PH on mouse, rat, rabbit, swine, sheep, and dog animal models (e.g., [133–138]). In addition to species, strain is also important in choosing the right model as revealed by the differences between the Wistar and Sprague-Dawley rats [139]. There are several methods to induce PH in animal models, the most popular being subcutaneous injection with monocrotaline (MCT), an alkaloid first extracted from the pea plan *Crotalaria spectabilis* [140] and hypobaric hypoxia [141] like at living at high altitude [142].

We [143] have used three PH models developed on 150–175g Sprague-Dawley rats purchased from Charles River Laboratories (Wilmington, MA, USA) under NYMC IACUC approved protocol. The models were obtained by: 1) subcutaneous injecting 6 weeks old males with single 40 mg/kg monocrotaline (MCT), or 2) by keeping them for 4 weeks in hypobaric (380 mmHg) hypoxia (10% oxygen), or 3) by applying both monocrotaline injection and hypobaric hypoxia. The experiments

 doi:10.20944/preprints202605.0124.v1

were performed at New York Medical College with the approval of the local IACUC on four groups of 4 rats each: CO (normal atmospheric conditions no MCT), HO (hypoxia but no MCT), CM (normal atmospheric conditions + MCT), HM (hypoxia + MCT). All three models exhibited decreased weight gain, hypertrophy and systolic pressure increase of the right ventricle, and medial wall thickening. As expected, the most severe PH manifestations occurred when both MCT and hypobaric hypoxia were applied (CM group) with neointima formation and occlusion of artery lumen [143]. Moreover, we reported [144] altered levels of Ngf (nerve growth factor), Nfe2l2 (nuclear factor erythroid-derived 2-like 2), and Slc2a1 (glucose transporter solute carrier family 2).

4.3.2. Lung Transcriptomic Consequences of Pulmonary Hypertension

All three models exhibited substantial alterations of the expression profiles of genes included in the KEGG-determined: chemokine signaling [116], vascular smooth muscle contraction [145], cell-cycle [94], and glycolysis/gluconeogenesis [46, citrate cycle [146] and fructose and manose [147] metabolism pathways. PH had a strong effect on the immune inflammatory gene network. However, the effects are not uniform among the models. For instance, HO turned the significant synergistic expression of *Ccl21* and *Ccl9* in control rats into a significant antagonistic expression, while CM and HM had no significant effect on the expression correlation of these two genes. Overall, the transcriptomic distance (defined by equation 7) with respect to CO of the three models were: 55.13 (CM), 62.84 (HO) and 91.10 (HM) [144].

4.4. Metabolic Syndrome

People affected by metabolic syndrome (MetS) [148,149] are obese (men waist circumference > 102 cm, women >90 cm), have elevated blood pressure (≥ 130/85 mmHg), triglycerides (≥150 mg/dL) and fasting glucose (≥ 100 mg/dL), but reduced high density lipids (men < 40 mg/dL, women (< 50 mg/dL. Experimental evidence blames the high fructose from the corn syrup and other sweets for the increasing incidence of MS [150,151]. In addition to MS, high fructose diet results also in hypertension [152,153], intra-cranial atherosclerosis [154], hyperurecimia [155], and dyslipidemia [156].

4.4.1. Induction of Metabolic Syndrome in a Dog Model

Currently there are several animal models of MetS, including Ossabaw and Göttingen minipigs [157], C57Bl'6j mice [158], Wistar and Sprague Dawley rats [158–160] and several dog strains (20 mentioned in [161]). In our studies, MetS was induced in six adult mongrel male dogs by including in their diet 60% isocaloric fructose for seven weeks owing to the certified impact of such diet [162,163]. Coronary blood flow, mean coronary flow, systolic (SBB) and diastolic (DBP) blood pressures, mean arterial pressure, end-diastolic pressure (LVEP) and rate of the left ventricle pressure rise were measured weekly and reported to the hemodynamic features at the start of fructose diet. Hemodynamics measurements were complemented with echocardiographic determination of the heart rate, stroke volume and left ventricle diameter in both systole and diastole, and blood concentrations of insulin (INS), angiotensin II (ANG II), uric acid (UA), homocysteine (HC), high (HDL) and low (LDL) density lipids [164].

4.4.2. Progression of the Metabolic Syndrome

The initial (reference) values were: SBP = 123 ± 4 mmHg, DBM = 83 ± 8 mmHg, LVEP = 4.4 ± 0.5 mmHG, LDL = 71 ± 3 mg/dL, INS = 12.1 ± 3.5 μM/mL, ANG II = 5.9 ± 1.5 pM/mL, HC = 7.8 ± 4.1, UA = 1.2 ± 0.4 mg/dL. After seven weeks, we found increased cardiac weight, altered dobutamine inotropic response and shifted the cardiac substrate utilization toward carbohydrate metabolism from 13.5 ± 3.8% of ATP production to 47.4 ± 4.0%. The dimensionless standard scores z of the three most affected features after seven weeks were: $z_{INS} = 13.71$, $z_{SBB} = 8.42$, $z_{LDL/HDL} = 7.53$. Figure 3 presents the evolution of the patholog (computed with formula 13) during the entire seven weeks high fructose diet as resulted from quantifying 15 studied characteristics.

 doi:10.20944/preprints202605.0124.v1

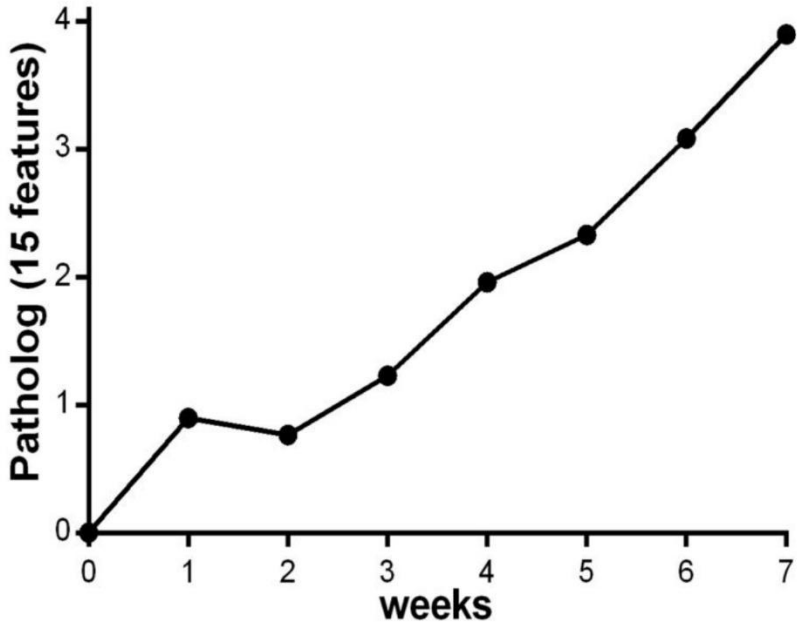

Figure 3. Evolution of the "patholog" associated to 15 features during the seven weeks high fructose feeding. Note that although according to pathophysiology observations, the metabolic syndrome was installed after 4 weeks of high fructose feeding, the "patholog" doubled after next 3 weeks fructose and continues to increase without any indication of saturation.

Moreover, we identified positive correlations between the seven weeks dynamics of SBP and INS (COR = 0.817), LDL/HDL and INS (COR = 0.821), SBP and DBP (COR = 0.810), HC and SBP (COR = 0.812), UA and INS (COR = 0.810), and HC and INS (COR = 0.831). The statistical significance of these correlations (from p-value = 0.025 for COR = 0.810 to p-value = 0.20 for COR = 0.831) indicate strong inter-conditioning of the considered characteristics.

4. Discussion

Decades of experimental studies of cardiovascular diseases molecular mechanisms on animal models taught us about the advantages but also the limitations of such models. We have been involved in all stages of gene expression studies: technology development, taking care of animal colonies and cell cultures, performing experiments with several platforms and in-house optimized wet protocols, developing mathematically advanced algorithms and computer software, and completing bioinformatics analyses. Moreover, we developed a mathematical approach to make comparable pathophysiological features of a wide diversity.

We proved that in addition to the strain of the infecting parasite, the animal species, strain, sex, age, hormonal status, heart chamber, diet and atmospheric conditions are important transcriptomic regulators. All these factors should be considered when translating the findings in the animal model to human diseases. Although originated in Latin America, Chagas disease is now present in: Australia, China, France, India, Indonesia, Italy, Japan, Portugal, Spain, UK, and U.S.A. [165]

Our finding of the down-regulation of *Gja1* in Chagas disease [96] complements other reports of the impact on the heart rhythm [166,167] and other cardiac diseases [168] of the deficiency of Connexin43 that it encodes. The effects of *Gja1* expression alteration might be explained by this gene controlling multiple functional pathways [169].

Most animal studies of the cardiac infarction were carried out on Wistar and Sprague-Dawley rats [170], although genetically engineered C57BL/6j mice (by knocking out *ApoE, Ldlr,* or *Srbi* genes) were also used in numerous studies [171]. Nevertheless, each model accounts for certain features of the human disease and might shred light on the responsible molecular mechanisms.

 doi:10.20944/preprints202605.0124.v1

Altered levels of Ngf, Nfe2l2 and Slc2a1 in pulmonary hypertension justifies the choice of Ngf as a potential PH therapeutic target [172], the cellular protection role of Nfe2l2 [173], and the importance of Slc2a1 for response to hypoxia [174]. A significant limitation of our study is the use of only male rats although PH is more frequent in women [175], most likely because of the hormonal status.

Although considered in many experimental studies, simulation of the metabolic syndrome in dogs raised several issues, including the lack of fasting hyperglycemia and atherogenic hyperlipidaemia in obese dogs [176]. Anyhow, we consider that a complex condition like MetS is better characterized by replacing the natural parameters with dimensionless standard scores and quantify it evolution with what we termed "patholog".

5. Conclusions

Although affected by numerous limitations, the animal models are still essential tools for deciphering the molecular mechanisms of the cardiovascular diseases.

Author Contributions: Conceptualization, D.A.I. and D.D.; methodology, D.A.I.; software, D.A.I.; validation, D.A.I., and D.D.; formal analysis, D.A.I.; investigation, D.A.I.; resources, D.A.I. and D.D.; data curation, D.A.I..; writing—original draft preparation, D.A.I.; writing—review and editing, D.D.; visualization, D.A.I.; supervision, D.D.; project administration, D.A.I.; funding acquisition, D.D. Both authors have read and agreed to the published version of the manuscript.

Funding: This research received no external funding.

Institutional Review Board Statement: Every animal study protocol was approved at the time by the Institutional Review Board of the collaborating academic institution: Albert Einstein College of Medicine, New York Medical College, Universidade Federal do Rio de Janeiro, or Yale University.

Informed Consent Statement: Not applicable.

Data Availability Statement: For each study, we provided the corresponding link to the NCBI Gene Expression Omnibus. We encourage all authors of articles published in MDPI journals to share their research data. In this section, please provide details regarding where data supporting reported results can be found, including links to publicly archived datasets analyzed or generated during the study. Where no new data were created, or where data is unavailable due to privacy or ethical restrictions, a statement is still required. Suggested Data Availability Statements are available in section "MDPI Research Data Policies" at https://www.mdpi.com/ethics.

Conflicts of Interest: The authors declare no conflicts of interest.

Abbreviations

The following abbreviations are used in this manuscript:

AECOM	Albert Einstein College of Medicine
AVE	Average normalized expression level of a gene
CCC	Chronic Chagas Cardiomyopathy
CCH	Chronic Constant Hypoxia
CHF	Congestive Heart Failure
CIH	Chronic Intermittent Hypoxia
CRE	Creatinine
COORD	percent of statistically synergistically expressed gene pairs + percent of antagonistically expressed pairs minus percent of independently expressed genes within the analyzed pathways
COR	pair-wise Pearson correlation coefficient of the (log2) of the normalized expression levels of two genes in the same condition/region
GCH	Gene Commanding Height
GLU	Blood sugar
IACUC	Institutional Animal Care and Use Committee

 doi:10.20944/preprints202605.0124.v1

KEGG	Kyoto Encyclopedia of Genes and Genomes
MetS	Metabolic Syndrome
P	Patholog
PH	Pulmonary Hypertension
PRE	Pathway Restoration Efficiency
PWR	Pair-Wise Relevance
REC	Relative Expression Control
REV	Relative Expression Variation
TD	Transcriptomic Distance
TRE	Transcriptomic Recovery Efficiency
TSH	thyroid stimulating hormone
WIR	Weighted Individual (Gene) Regulation
WPR	Weighted Pathway Regulation

References

1. Albu, M.; Sedmera, D.; Stainier, D.Y.R. Recent insights into atrial chamber formation. *Semin Cell Dev Biol.* **2025**; 175:103664. https://doi.org/10.1016/j.semcdb.2025.103664.
2. Stephenson, A.; Adams, J.W.; Vaccarezza, M. The vertebrate heart: an evolutionary perspective. *J Anat.* **2017**; 231(6):787-797. https://doi.org/10.1111/joa.12687.
3. Kiani, A.K.; Pheby, D.; Henehan, G.; Brown, R.; Sieving, P.; Sykora, P. et al.; INTERNATIONAL BIOETHICS STUDY GROUP. Ethical considerations regarding animal experimentation. *J Prev Med Hyg*. **2022.** 7;63(2 Suppl 3):E255-E266. https://doi.org/10.15167/2421-4248/jpmh2022.63.2S3.2768.
4. National Research Council. Guide for the care and use of laboratory animals. 8th Edition. Washington D.C. The National Academies Press. Available online at: https://grants.nih.gov/grants/olaw/guide-for-the-care-and-use-of-laboratory-animals.pdf. Accessed 01/31/2026.
5. Vo, Q.D. Gene editing therapy as a therapeutic approach for cardiovascular diseases in animal models: A scoping review. *PLoS One*. **2025**; 20(6):e0325330. https://doi.org/10.1371/journal.pone.0325330.
6. Zeng, L.; Chi, J.; Zhu, M.; Hao, H.; Long, S.; Liu, Z.; Zhang, C. Rodent Models for Atherosclerosis. *Int J Mol Sci.* **2025**; 27(1):378. https://doi.org/10.3390/ijms27010378.
7. Zeng, L.; Chi, J.; Zhu, M.; Hao, H.; Long, S.; Liu, Z. et al. Rodent Models for Atherosclerosis. *Int J Mol Sci*. **2025**; 27(1):378. https://doi.org/10.3390/ijms27010378.
8. Delfos, L.; Huis, C.; Imani, N.; Roeters van Lennep, J.E.; Hooijmans, C.R.; Bot, I. Modulation of IL-1, IL-6 and IL-18 cytokine signaling in animal models of atherosclerosis: a systematic review evaluating animal sex in preclinical research. *Eur J Pharmacol*. **2025**; 1008:178336. https://doi.org/10.1016/j.ejphar.2025.178336.
9. Wu, X.; Zhou, Q.; Huang, Y.; Jiang, W.; Zhou, J.; Qian, K. et al. Cellular senescence in age-related cardiovascular disease: past and future. *Front Aging.* **2026**; 6:1721744. https://doi.org/10.3389/fragi.2025.1721744.
10. Zulkefli, S.B.; Mohamad, F.; Nasir, N.A.A.; Shuid, A.N.; Azme, N. Mechanistic Insights into Therapeutic Strategies for Post- Menopausal Atherosclerosis: Evidence from an Ovariectomized Mouse Model. *J Cardiovasc Transl Res*. **2026**; 19(1):46. https://doi.org/10.1007/s12265-026-10766-8.
11. Enkhmaa, B.; Anuurad, E.; Berglund, L. Mediterranean diet and cardiovascular disease: a step closer to mechanisms using a precision animal model? *Transl Res*. **2015**; 166(1):41-3. https://doi.org/10.1016/j.trsl.2015.01.011.
12. Sun, Y.; Su, Y.; Ding, N.; Yang, Z.; Zhao, J.; Wang, X. et al. Effect of Yi-Nao-Jie-Yu Prescription on Post-Stroke Depression in Rats using Middle Cerebral Artery Occlusion Combined with Behavioral Restraint. *J Vis Exp*. **2026**; (227). https://doi.org/10.3791/69537.
13. Chege, B.M.; Mwangi, P.W.; Githinji, C.G.; Bukachi, F. Combined antiretroviral therapy with low- or normal-protein, high-calorie diets appears to induce significant deleterious electrocardiographic changes in a rodent model. *Braz J Med Biol Res*. **2026**; 59:e14744. https://doi.org/10.1590/1414-431X2026e14744.
14. Zheng, X.; Li, Y.; Wang, P.; Guo, Z.; Liu, Y.; Liu, Q. et al. Physical exercise mitigates chronic psychological stress-induced vascular inflammation via the BDNF-Kif4-TARM1 axis. *Clin Transl Med*. **2026**; 16(4):e70674. https://doi.org/10.1002/ctm2.70674.

 doi:10.20944/preprints202605.0124.v1

15. Mohan, A.S.; Radhakrishnan, S.; Aswany, M. G.; Mohan, N.; John, A.J.; Anie Y. Cl-amidine attenuates neutrophil extracellular trap-enclosed extracellular vesicle (NET-EV)-mediated thrombosis in diabetic mice. *Thromb Res*. **2026**; 260:109658. https://doi.org/10.1016/j.thromres.2026.109658.
16. Duke. Mouse and rat microarrays. Available online at: https://www.ncbi.nlm.nih.gov/geo/query/acc.cgi?acc=GPL9207, https://www.ncbi.nlm.nih.gov/geo/query/acc.cgi?acc=GPL8928, https://www.ncbi.nlm.nih.gov/geo/query/acc.cgi?acc=GPL8938. Accessed 01/31/2026.
17. AECOM. Mouse and rat cDNA and oligonucleotide microarray printed by the Microarray Facility of Albert Einstein College of Medicine. Available on line at: https://www.ncbi.nlm.nih.gov/geo/query/acc.cgi?acc=GPL369, GPL1698, GPL5371. Accessed 01/31/2026.
18. Yale. Mouse microarrays. Available online at: https://www.ncbi.nlm.nih.gov/geo/query/acc.cgi?acc=GPL2828. Accessed 01/31/2026.
19. Agilent technology. SurePrint Microarray Hybridization Setup. Available online at: https://www.youtube.com/watch?v=AgWbneDtVXU. Accessed 01/31/2026.
20. Iacobas, D.A.; Obiomon, E.A.; Iacobas, S. Genomic Fabrics of the Excretory System's Functional Pathways Remodeled in Clear Cell Renal Cell Carcinoma. *Curr. Issues Mol. Biol.* **2023**, *45*, 9471-9499. https://doi.org/10.3390/cimb45120594.
21. Iacobas, S.; Ede, N.; Iacobas, D.A. The Gene Master Regulators (GMR) Approach Provides Legitimate Targets for Personalized, Time-Sensitive Cancer Gene Therapy. *Genes (Basel)*. **2019**; 10(8):560. https://doi.org/10.3390/genes10080560
22. Fan, C.; Iacobas, D.A.; Zhou, D.; Chen, Q.; Lai, J.K.; Gavrialov, O.; Haddad, G.G. Gene expression and phenotypic characterization of mouse heart after chronic constant or intermittent hypoxia. *Physiol Genomics*. **2005**; 22(3):292-307. https://doi.org/10.1152/physiolgenomics.00217.2004.
23. KEGG. Kyoto Encyclopedia of Genes and Genomes. Available on line at: https://www.kegg.jp/kegg/pathway.html. Accessed 01/31/2026.
24. Nganele DM, Hintze TH. Cardiac chemical reflex control of preload in conscious dogs. *Am J Physiol*. **1990**; 258(4 Pt 2):H1055-63.
25. Iacobas, D.A. *Medical Biostatistics*, 3rd English ed.; Bucura Mond: Bucarest, Romania, 1997; ISBN 973-97977-3-3.
26. Gene Expression Omnibus. Sex-dependent gene regulatory networks of the heart rhythm. Available online at: https://www.ncbi.nlm.nih.gov/geo/query/acc.cgi?acc=GSE17324. Accessed March 1st, 2026
27. Iacobas, D.A.; Iacobas, S.; Thomas, N.; Spray, D.C. Sex-dependent gene regulatory networks of the heart rhythm. *Funct Integr Genomics*. **2010**; 10(1):73-86. https://doi.org/10.1007/s10142-009-0137-8.
28. Cellini, A.; Höfler, D.; Arias-Loza, P.A.; Bandleon, S.; Langsenlehner, T.; Kohlhaas, M. et al. The α2-isoform of the Na+/K+-ATPase protects against pathological remodeling and β-adrenergic desensitization after myocardial infarction. *Am J Physiol Heart Circ Physiol.* **2021**; 321(4):H650-H662. https://doi.org/10.1152/ajpheart.00808.2020.
29. Hutschalik, T.; Dasí, A.; Riebel, L.L.; Wiendels, M.; Bakker, F.; Beckers, L.J.A.M. et al. GJA5 and ATP1A1 perturbations recapitulate inflammation-related beat irregularities in iPSC-based atrial myocardium tissue model. *Front Immunol.* **2026**; 16:1719392. https://doi.org/10.3389/fimmu.2025.1719392.
30. Ying, H.; Fan, H.; Wang, Y.; Jiang, R.; Cai, D.; Cheng, H. et al. Connexin43 Deficiency Leads to Ventricular Arrhythmias by Reprogramming Proline Metabolism. *Adv Sci (Weinh)*. **2026**; 13(19):e16090. https://doi.org/10.1002/advs.202516090.
31. James, A.F.; Choisy, S.C.; Hancox, J.C. Recent advances in understanding sex differences in cardiac repolarization. *Prog Biophys Mol Biol.* **2007**; 94(3):265-319. https://doi.org/10.1016/j.pbiomolbio.2005.05.010.
32. Jonsson, M.K.; Vos, M.A.; Duker, G.; Demolombe, S.; van Veen, T.A. Gender disparity in cardiac electrophysiology: implications for cardiac safety pharmacology. *Pharmacol Ther*. **2010**; 127(1):9-18. https://doi.org/10.1016/j.pharmthera.2010.04.002.
33. Burke, J.H.; Ehlert, F.A.; Kruse, J.T.; Parker, M.A.; Goldberger, J.J.; Kadish, A.H. Gender-specific differences in the QT interval and the effect of autonomic tone and menstrual cycle in healthy adults. *Am J Cardiol*. **1997** 79(2):178-81. https://doi.org/10.1016/s0002-9149(96)00707-2.

 doi:10.20944/preprints202605.0124.v1

34. Gene Expression Omnibus. Gene expression and phenotypic characterization of mouse heart after chronic constant or intermittent hypoxia. Available online at: https://www.ncbi.nlm.nih.gov/geo/query/acc.cgi?acc=GSE2271. Accessed March 1st, 2026
35. Agilent-026655. Whole Mouse Genome Microarray 4x44K v2. Available online at: https://www.ncbi.nlm.nih.gov/geo/query/acc.cgi?acc=GPL10333. Accessed Feb. 20/2026
36. Gene Expression Omnibus. Left-right transcriptomic differences in adult male mouse heart ventricles. Available online at: https://www.ncbi.nlm.nih.gov/geo/query/acc.cgi?acc=GSE45348. Accessed Feb. 20/2026
37. Gene Expression Omnibus. Left-right transcriptomic differences in adult male mouse heart atria. Available online at: https://www.ncbi.nlm.nih.gov/geo/query/acc.cgi?acc=GSE45339. Accessed Feb. 20/2026
38. Iacobas, S.; Amuzescu, B.; Iacobas, D.A. Transcriptomic uniqueness and commonality of the ion channels and transporters in the four heart chambers. *Sci Rep*. **2021**; 11(1):2743. https://doi.org/10.1038/s41598-021-82383-1.
39. Artemieva, M.M.; Makeeva, A.V.; Adasheva, D.A.; Shein, V.E.; Katrukha, A.G.; Postnikov AB. et al. Left Ventricular and Right Ventricular Hypertrophy Modelling to Study PAPP-A-Mediated IGFBP-4 Cleavage-a Mechanism That Regulates IGF Bioavailability in Adult Rats. *Int J Mol Sci*. **2026**; 27(6):2761. https://doi.org/10.3390/ijms27062761.
40. Wing-Ki Chik, B.; Chan, K.L.; Chow, P.C.; Kwong-Man Yu, C.; Yuk-Ting Chan, Y.; Cheung, Y.F. Right Atrial Functional Reserve is Associated With Right Ventricular Diastolic Reserve and Liver Stiffness in Repaired Tetralogy of Fallot. *Echocardiography*. **2026**; 43(3):e70426. https://doi.org/10.1111/echo.70426.
41. Zang, H.; Jia, C.; Pan, Y.; Li, X.; Zhang, Q. Left Atrial Volume Index and Left Ventricular Mass Index Determine the Benefits of Spironolactone in Patients With Heart Failure With Preserved Ejection Fraction. *J Am Heart Assoc*. **2026**; 15(7):e044115. https://doi.org/10.1161/JAHA.125.044115.
42. Günthel, M.; Barnett, P.; Christoffels, V.M. Development, Proliferation, and Growth of the Mammalian Heart. *Mol Ther*. **2018**; 26(7):1599-1609. https://doi.org/10.1016/j.ymthe.2018.05.022.
43. KEGG. Adrenergic signaling in cardiomyocytes. https://www.kegg.jp/pathway/mmu04261. Accessed March 1st, 2026
44. KEGG. Calcium signaling pathway. https://www.kegg.jp/pathway/mmu04020. Accessed March 1st, 2026
45. KEGG. Cardiac muscle contraction. https://www.kegg.jp/pathway/mmu04260. Accessed March 1st, 2026
46. KEGG. Glycolysis/Gluconeogenesis. https://www.kegg.jp/pathway/mmu00010. Accessed March 1st, 2026
47. KEGG. Oxidative Phosphorylation. https://www.kegg.jp/pathway/mmu00190. Accessed March 1st, 2026
48. Thomas NM, Jasmin JF, Lisanti MP, Iacobas DA. Sex differences in expression and subcellular localization of heart rhythm determinant proteins. *Biochem Biophys Res Commun*. **2011**; 406(1):117-22. https://doi.org/10.1016/j.bbrc.2011.02.006.
49. Nelson, J.F.; Felicio, L.S.; Randall, P.K.; Sims, C.; Finch, C.E. A longitudinal study of estrous cyclicity in aging C57BL/6J mice: I. Cycle frequency, length and vaginal cytology. *Biol Reprod*. **1982**; 27(2):327-39. https://doi.org/10.1095/biolreprod27.2.327.
50. Musil, L.S.; Goodenough, D.A. Biochemical analysis of connexin43 intracellular transport, phosphorylation, and assembly into gap junctional plaques. *J Cell Biol*. **1991**; 115(5):1357-74. https://doi.org/10.1083/jcb.115.5.1357.
51. Harvey, B.I.; Yoniles, A.M.; Monsivais, A.; Du, J.; Zadorozny, L.; Yu, Q. et al. Sex-Specific Differences in LPS-Induced Rapid Myocardial Dysfunction. *Int J Mol Sci*. **2025**; 26(13):5963. https://doi.org/10.3390/ijms26135963.
52. Turner, C.G.; DuPont, J.J. The effect of transient sex hormone fluctuations on vascular endothelial function. *Am J Physiol Heart Circ Physiol*. **2025**; 329(1):H217-H232. https://doi.org/10.1152/ajpheart.00174.2025.
53. Lichtenstein, A.H.; Khera, A.; Anderson, C.A.M.; Appel, L.J.; DeSilva, D.M.; Gardner, C. et al.; American Heart Association. 2026 Dietary Guidance to Improve Cardiovascular Health: A Scientific Statement From the American Heart Association. *Circulation*. **2026**. https://doi.org/10.1161/CIR.0000000000001435. Epub ahead of print.
54. Gene Expression Omnibus. Transcriptomic Effects of Law Salt Diet on the Mouse Left Ventricle. Available online: https://www.ncbi.nlm.nih.gov/geo/query/acc.cgi?acc=GSE72561 (accessed on 27 January 2026).

 doi:10.20944/preprints202605.0124.v1

55. KEGG Pathways. Fatty acid Biosynthesis. Available online: https://www.genome.jp/kegg-bin/show_pathway?mmu00061. Accessed on 11 January 2026.
56. KEGG Pathways. Steroid Biosynthesis. Available online: https://www.genome.jp/kegg-bin/show_pathway?mmu00100. Aaccessed on 11 January 2026.
57. Iacobas, D.A.; Allen, H.; Iacobas, S. Low-Salt Diet Regulates the Metabolic and Signal Transduction Genomic Fabrics, and Remodels the Cardiac Normal and Chronic Pathological Pathways. *Curr. Issues Mol. Biol.* **2024**, *46*, 2355-2385. https://doi.org/10.3390/cimb46030150
58. KEGG pathway. Chagas disease. Available online at: https://www.kegg.jp/kegg-bin/show_pathway?mmu05142. Accessed on March 1, 2026.
59. KEGG Pathways. Diabetic cardiomyopathy. Available online at: https://www.kegg.jp/kegg-bin/show_pathway?mmu05415. Accessed on March 1, 2026.
60. KEGG Pathways. Dilated cardiomyopathy. Available online at: https://www.kegg.jp/kegg-bin/show_pathway?mmu05414. Accessed on March 1, 2026.
61. KEGG Pathways. Hypertrophic cardiomyopathy. Available online at: https://www.kegg.jp/kegg-bin/show_pathway?mmu05410. Accessed on March 1, 2026.
62. Iacobas, D.A.; Fan, C.; Iacobas, S.; Haddad, G.G. Integrated transcriptomic response to cardiac chronic hypoxia: translation regulators and response to stress in cell survival. *Funct Integr Genomics*. **2008**; 8(3):265-75. https://doi.org/10.1007/s10142-008-0082-y.
63. Penaloza, D.; Arias-Stella, J. The heart and pulmonary circulation at high altitudes: healthy highlanders and chronic mountain sickness. *Circulation*. **2007**; 115(9):1132–1146. https://doi.org/10.1161/CIRCULATIONAHA.106.624544. Review.
64. Covello K.L.; Simon, M.C. HIFs, hypoxia, and vascular development. *Curr Top Dev Biol*. **2004**; 62:37–54. https://doi.org/10.1016/S0070-2153(04)62002-3. Review.
65. Macario, A.J. Heat-shock proteins and molecular chaperones: implications for pathogenesis, diagnostics, and therapeutics. *Int J Clin Lab Res.* **1995**; 25(2):59-70. https://doi.org/10.1007/BF02592359.
66. Dursunoglu, D.; Dursunoglu, N. Cardiovascular diseases in obstructive sleep apnea. *Tuberk Toraks*. **2006**; 54(4):382–396. Review.
67. Park, A.M.; Nagase, H.; Kumar, S.V.; Suzuki, Y.J. Effects of intermittent hypoxia on the heart. *Antioxid Redox Signal*. **2007**; 9(6):723–729. https://doi.org/10.1089/ars.2007.1460. Review.
68. Jain, V. Clinical perspective of obstructive sleep apnea-induced cardiovascular complications. *Antioxid Redox Signal*. **2007**; 9(6):701–710. https://doi.org/10.1089/ars.2007.1558. Review.
69. Iacobas, S.; Iacobas D.A. Effects of chronic intermittent hypoxia on cardiac rhythm transcriptomic networks. In: *Intermittent Hypoxia and Human Diseases*, L. Xi, T.V. Serebrovskaya, Eds.; Springer-Verlag London UK; 2012, pp. 15-27.
70. Uniacke, J.; Holterman, C.; Lachance, G. et al. An oxygen-regulated switch in the protein synthesis machinery. *Nature* **2012,** 486, 126–129. https://doi.org/10.1038/nature11055
71. Iacobas DA, Iacobas S, Haddad GG. Heart rhythm genomic fabric in hypoxia. Biochem Biophys Res Commun. 2010 Jan 22;391(4):1769-74. https://doi.org/10.1016/j.bbrc.2009.12.151.
72. KEGG pathway. Calcium signaling pathway. Available online at: https://www.kegg.jp/pathway/mmu04020. Accessed on March 1st, 2026.
73. KEGG pathway. WNT signaling pathway. Available at: https://www.kegg.jp/kegg-bin/show_pathway?mmu04310. Accessed on March 2nd, 2026.
74. de Lima, E.V.; Bertolini, V.K.D.S.; Cunha, M.D.P.; Miguel, D.C.; de Almeida, E.A.; Gadelha, F.R. Trypanosoma cruzi DTU diversity, benznidazole response, and clinical manifestations of Chagas disease: a seventeen-year systematic review and meta-analysis. *Acta Trop.* **2026**: 108105. https://doi.org/10.1016/j.actatropica.2026.108105. Epub ahead of print.
75. Agudelo Higuita, N.I.; Henao-Martínez, A.F.; Vieira Batista, M.; Herrera Bernal, C.P.; Rezende Filho, J.; Rassi, A. Jr. State-of-the-Art Review: Chagas Disease-an Enduring Challenge. *Clin Infect Dis*. **2026**; 82(2):187-205. https://doi.org/10.1093/cid/ciaf654.

 doi:10.20944/preprints202605.0124.v1

76. Tanowitz, H.B.; Machado, F.S.; Jelicks, L.A.; Shirani, J.; de Carvalho, A.C.C.; Spray, D.C. et al. Perspectives on Trypanosoma cruzi–Induced Heart Disease (Chagas Disease). *Progress in Cardiovascular Diseases*. **2009;** 51:524–539.
77. Barbosa, J.M.C.; Duarte, R.B.; Veloso, H.H.; Daliry, A.; Salomão, K. Chagas disease and amiodarone: a bibliometric and systematic review from cell to patient. *Front Pharmacol*. **2026**; 17:1749345. https://doi.org/10.3389/fphar.2026.1749345.
78. Gonzaga, B.M.S.; Ferreira, R.R.; Coelho, L.L.; Carvalho, A.C.C.;, Garzoni, L.R.; Araujo-Jorge, T.C. Clinical trials for Chagas disease: etiological and pathophysiological treatment. *Front Microbiol*. **2023**; 14:1295017. https://doi.org/10.3389/fmicb.2023.1295017.
79. Mukherjee, S.; Belbin, T.J.; Spray, D.C.; Iacobas, D.A.; Weiss, L.M.; Kitsis, R.N. et al. Microarray analysis of changes in gene expression in a murine model of chronic chagasic cardiomyopathy. *Parasitol Res*. **2003**; 91(3):187-96. https://doi.org/10.1007/s00436-003-0937-z.
80. Adesse, D.; Iacobas, D.A.; Iacobas, S.; Garzoni, L.R.; Meirelles Mde, N.; Tanowitz, H.B. et al. Transcriptomic signatures of alterations in a myoblast cell line infected with four distinct strains of Trypanosoma cruzi. *Am J Trop Med Hyg*. **2010**; 82(5):846-54. https://doi.org/10.4269/ajtmh.2010.09-0399.
81. Gene Expression Omnibus. Transcriptomic alterations in a myoblast cell line infected with four distinct strains of Trypanosoma cruzi. Available online at: https://www.ncbi.nlm.nih.gov/geo/query/acc.cgi?acc=GSE18175. Accessed on March 1st. 2026
82. Soares, M.B.; de Lima, R.S.; Rocha, L.L.; Vasconcelos, J.F.; Rogatto, S.R.; dos Santos, R.R. et al. Gene expression changes associated with myocarditis and fibrosis in hearts of mice with chronic chagasic cardiomyopathy. *J Infect Dis*. **2010**; 202(3):416-26. https://doi.org/10.1086/653481.
83. Gene Expression Omnibus. Gene expression changes associated with myocarditis and fibrosis in hearts of mice with chronic chagasic cardiomyopathy. Available online at: https://www.ncbi.nlm.nih.gov/geo/query/acc.cgi?acc=GSE17363. Accessed on March 1st, 2026.
84. Goldenberg, R.C.; Iacobas, D.A.; Iacobas, S.; Rocha, L.L.; da Silva de Azevedo Fortes, F.; Vairo, L. et al. Transcriptomic alterations in Trypanosoma cruzi-infected cardiac myocytes. *Microbes Infect*. **2009**; 11(14-15):1140-9. https://doi.org/10.1016/j.micinf.2009.08.009.
85. Gene Expression Omnibus. Transcriptomic alterations in Trypanosoma cruzi-infected cardiac myocytes. Available online at: https://www.ncbi.nlm.nih.gov/geo/query/acc.cgi?acc=GSE17330. Accessed on March 1st, 2026.
86. Machado, R.R.B.; B Scariot, D.; Bakoshi, A.B.K.; Mbaye, E.H.A.; Almunif, S.; Sharma, S. et al. Cytosolic Delivery of a Bithiophene Derivative via Polymersomes Kills Trypanosoma cruzi Amastigotes and Modulates the Inflammatory Response. *ACS Appl Nano Mater*. **2026**; 9(8):3689-3703. https://doi.org/10.1021/acsanm.5c05104.
87. da Silva, G.P.; Sousa, L.R.D.; Vieira, P.M.A.; Stefani, R.; do Nascimento, A.M. In Vitro and In Silico Evaluation of the Trypanocidal Activity of a Subfraction Isolated from Mutisia campanulata. *ACS Omega*. **2026**; 11(5):7659-7671. https://doi.org/10.1021/acsomega.5c08989.
88. Lanera, S.D.C.; Lara, L.D.S.; Orlando, L.M.R.; de Souza, T.P.; de Oliveira, E.C.; Paes, V.B. et al. Trypanosoma cruzi carbonic anhydrase inhibitors as a potential antiparasitic agent. *Int J Biol Macromol*. **2026**; 351:150985. https://doi.org/10.1016/j.ijbiomac.2026.150985.
89. Prado, C.M.; Fine, E.J.; Koba, W.; Zhao, D.; Rossi, M.A.; Tanowitz, H.B. et al. Micropositron emission tomography in the evaluation of Trypanosoma cruzi-induced heart disease: Comparison with other modalities. *Am J Trop Med Hyg*. **2009;** 81:900-5.
90. de Souza, A.P.; Tang, B.; Tanowitz, H.B.; Araujo-Jorge, T.C.; Jelicks, E.L. Magnetic resonance imaging in experimental Chagas disease: a brief review of the utility of the method for monitoring right ventricular chamber dilation. *Parasitol Res*. **2005;** 97:87-90.
91. Jelicks, L.A.; Tanowitz, H.B. Advances in imaging of animal models of Chagas disease. *Adv Parasitol*. **2011**; 75:193-208. https://doi.org/10.1016/B978-0-12-385863-4.00009-5.
92. Seah, S.K.; Marsden, P.D.; Voller, A.; Pettitt, L.E. Experimental Trypanosoma cruzi infection in rhesus monkeys--the acute phase. *Trans R Soc Trop Med Hyg*. **1974**; 68(1):63-9. https://doi.org/10.1016/0035-9203(74)90254-5.

 doi:10.20944/preprints202605.0124.v1

93. KEGG. JAK-STAT signaling pathway. Available online at: https://www.kegg.jp/pathway/mmu04630. Accessed on March 1st.
94. KEGG. Cell cycle. Available online at: https://www.kegg.jp/kegg-bin/show_pathway?mmu04110. Accessed on March 1st
95. Nisimura, L.M.; Coelho, L.L.; de Melo, T.G.; Vieira, P.C.; Victorino, P.H.; Garzonim L.R. et al. Trypanosoma cruzi Promotes Transcriptomic Remodeling of the JAK/STAT Signaling and Cell Cycle Pathways in Myoblasts. *Front Cell Infect Microbiol.* **2020**; 10:255. https://doi.org/10.3389/fcimb.2020.00255.
96. KEGG. Gap junction. Available at: https://www.kegg.jp/kegg-bin/show_pathway?mmu04540. Accessed on March 1st.
97. Adesse, D.; Goldenberg, R.C.; Fortes, F.S.; Jasmin, Iacobas, D.A.; Iacobas, S. et al. Gap junctions and chagas disease. *Adv Parasitol.* **2011**; 76:63-81. https://doi.org/10.1016/B978-0-12-385895-5.00003-7.
98. Iacobas, D.A.; Manzoor, S.; Daniels, D.; Iacobas, S.; Xi, L. Mitochondrial Collapse Responsible for Chagasic and Post-Ischemic Heart Failure Is Reversed by Cell Therapy Under Different Transcriptomic Topologies. *Curr. Issues Mol. Biol.* **2025**, *47*, 940. https://doi.org/10.3390/cimb47110940
99. Parker, A.M.; Lees, J.G.; Murray, A.J.; Velagic, A.; Lim, S.Y.; De Blasio, M.J.; Ritchie, R.H. Precision Medicine: Therapeutically Targeting Mitochondrial Alterations in Heart Failure. *JACC Basic Transl. Sci.* **2025**, 10, 101345. https://doi.org/10.1016/j.jacbts.2025.101345.
100. Mongelli, A.; Mengozzi, A.; Geiger, M.; Gorica, E.; Mohammed, S.A.; Paneni, F. et al. Mitochondrial epigenetics in aging and cardiovascular diseases. *Front. Cardiovasc. Med*. **2023**, 10, 1204483. https://doi.org/10.3389/fcvm.2023.1204483
101. Pietrangelo, D.; Lopa, C.; Litterio, M.; Cotugno, M.; Rubattu, S.; Lombardi, A. Metabolic Disturbances Involved in Cardiovascular Diseases: The Role of Mitochondrial Dysfunction, Altered Bioenergetics and Oxidative Stress. *Int. J. Mol. Sci*. **2025**, 26, 6791. https://doi.org/10.3390/ijms26146791.
102. Dhalla, N.S.; Ostadal, P.; Tappia, P.S. Involvement of Oxidative Stress in Mitochondrial Abnormalities During the Development of Heart Disease. *Biomedicines* **2025**, 13, 1338. https://doi.org/10.3390/biomedicines13061338
103. Pinto Dias, J.C. The treatment of Chagas disease (South American trypanosomiasis). *Ann Intern Med*. **2006**; 16;144:772-4.
104. Antonoglou, M.B.; Sánchez Alberti, A.; Redolfi, D.M.; Bivona, A.E.; Noli Truant, S.; Sarratea, M.B. et al. Protective immunity against Chagas disease induced by a superantigen-based chimeric DNA vaccine delivered by attenuated Salmonella. *Front Immunol*. **2026**; 17:1788924. https://doi.org/10.3389/fimmu.2026.1788924.
105. Sanchez Alberti, A.; Bivona, A.E.; Matos, M.N.; Cerny, N.; Schulze, K.; Weißmann, S. et al. Mucosal Heterologous Prime/Boost Vaccination Induces Polyfunctional Systemic Immunity, Improving Protection Against Trypanosoma cruzi. *Front Immunol*. **2020**; 11:128. https://doi.org/10.3389/fimmu.2020.00128
106. Cunha-Neto, E.; Santoro Rosa, D. Can Vaccination Prevent the Development of Chagas Disease Cardiomyopathy? *JACC Basic Transl Sci.* **2026**; 11(3):101513. https://doi.org/10.1016/j.jacbts.2026.101513.
107. Tejo, A.M.; Campos, S.V. Parasitic diseases in heart transplantation: challenges of Toxoplasmosis and Chagas Disease. *JHLT Open*. **2025**; 11:100450. https://doi.org/10.1016/j.jhlto.2025.100450.
108. Soares, M.B.; Lima, R.S.; Souza, B.S.; Vasconcelos, J.F.; Rocha, L.L.; Dos Santos, R.R. et al. Reversion of gene expression alterations in hearts of mice with chronic chagasic cardiomyopathy after transplantation of bone marrow cells. *Cell Cycle*. **2011**; 10(9):1448-55. https://doi.org/10.4161/cc.10.9.15487.
109. Barbash, I.M.; Chouraqui, P.; Baron, J.; Feinberg, M.S.; Etzion, S.; Tessone, A. et al. Systemic delivery of bone marrow-derived mesenchymal stem cells to the infarcted myocardium: feasibility, cell migration, and body distribution. *Circulation*. **2003**; 108(7):863–868. https://doi.org/10.1161/01.CIR.0000084828.50310.6A.
110. Campos de Carvalho, A.C.; Goldenberg, R.C.; Jelicks, L.A.; Soares, M.B.; Dos Santos, R.R.; Spray, D.C. et al. Cell Therapy in Chagas Disease. *Interdiscip Perspect Infect Dis*. **2009**; 2009:484358. https://doi.org/10.1155/2009/484358.
111. Sousa, M.G.; Paulino-Junior, D.; Pascon, J.P.; Pereira-Neto, G.B.; Carareto, R.; Champion T. et al. Cardiac function in dogs with chronic Chagas cardiomyopathy undergoing autologous stem cell transplantation into the coronary arteries. *Can Vet J.* **2011**; 52(8):869-74.

 doi:10.20944/preprints202605.0124.v1

112. Soares, M.B.; Santos, R.R. Current status and perspectives of cell therapy in Chagas disease. *Mem Inst Oswaldo Cruz*. **2009**; 104 Suppl 1:325-32. https://doi.org/10.1590/s0074-02762009000900043.
113. Jasmin, Torres, A.L.; Nunes, H.M.; Passipieri, J.A.; Jelicks, L.A.; Gasparetto, E.L. et al. Optimized labeling of bone marrow mesenchymal cells with superparamagnetic iron oxide nanoparticles and in vivo visualization by magnetic resonance imaging. *J Nanobiotechnology*. **2011**; 9:4. https://doi.org/10.1186/1477-3155-9-4.
114. Soares, M.B.; Lima, R.S.; Rocha, L.L.; Takyia, C.M.; Pontes-de-Carvalho, L.; de Carvalho, A.C. Et al. Transplanted bone marrow cells repair heart tissue and reduce myocarditis in chronic chagasic mice. *Am J Pathol.* **2004**; 164(2):441-7. https://doi.org/10.1016/s0002-9440(10)63134-3.
115. Iacobas, D.A.; Iacobas, S.; Tanowitz, H.B.; Campos de Carvalho, A.; Spray, D.C. Functional genomic fabrics are remodeled in a mouse model of Chagasic cardiomyopathy and restored following cell therapy. *Microbes Infect*. **2018**; 20(3):185-195. https://doi.org/10.1016/j.micinf.2017.11.003.
116. KEGG. Chemokine signaling pathway. Available online at: https://www.kegg.jp/pathway/mmu04062. Accessed on March 1st 2026.
117. Anversa, P.; Li, P.; Zhang, X.; Olivetti, G.; Capasso, J.M. Ischaemic myocardial injury and ventricular remodelling. *Cardiovasc Res*. **1993**; 27(2):145-57. https://doi.org/10.1093/cvr/27.2.145.
118. Sutton, M.G.; Sharpe, N. Left ventricular remodeling after myocardial infarction: pathophysiology and therapy. *Circulation*. **2000**;101:2981–2988. https://doi.org/10.1161/01.cir.101.25.2981.
119. Mehta, J.L.; Li, Y. Inflammation in ischemic heart disease: Response to tissue injury or a pathogenetic villain? *Cardiovascular Research*, **1999;** 43 (2), 291–299, https://doi.org/10.1016/S0008-6363(99)00132-7.
120. Lee, J.W.; Kang, E.J.; Hwang, S.H.; Kim, S.M. Cardiac CT for the Assessment of Ischemic Cardiomyopathy. *J Korean Soc Radiol.* **2026**; 87(2):181-197. https://doi.org/10.3348/jksr.2025.0125.
121. Lachtermacher, S.; Esporcatte, B.L.; Montalvão, F.; Costa, P.C.; Rodrigues, D.C.; Belem, L. et al. Cardiac gene expression and systemic cytokine profile are complementary in a murine model of post-ischemic heart failure. *Braz J Med Biol Res*. **2010**; 43(4):377-89. https://doi.org/10.1590/s0100-879x2010007500014.
122. Frasure-Smith, N.; Lespérance, F.; Talajic, M. Depression and 18-month prognosis after myocardial infarction. *Circulation.* **1995**; 91:999–1005. https://doi.org/10.1161/01.CIR.91.4.999.
123. Patel, P.; Yang, F.; Iacobas, D.A.; Xi, L. Mental disorders after myocardial infarction: potential mediator role for chemokines in heart-brain interaction? *J Geriatr Cardiol*. **2024**; 21(9):913-926. https://doi.org/10.26599/1671-5411.2024.09.004.
124. Indian, P.A.; Trivedi, M.V.; Gaikwad, A.B. Deciphering the role of mitochondrial cytochrome C oxidase subunit 4 in cardiac health and disease. *Life Sci*. **2026**; 391:124295. https://doi.org/10.1016/j.lfs.2026.124295. Epub 2026 Feb 26.
125. Kurian, G.A.; Gino, E.R. Strategic targeting of mitochondria in ischemic heart disease: mechanisms and emerging therapies. *Expert Rev Cardiovasc Ther.* **2026**; 24(3):185-205. https://doi.org/10.1080/14779072.2026.2637751.
126. Iacobas, D.A.; Xi, L. Theory and Applications of the (Cardio) Genomic Fabric Approach to Post-Ischemic and Hypoxia-Induced Heart Failure. *J. Pers. Med.* **2022**, *12*, 1246. https://doi.org/10.3390/jpm12081246
127. Lachtermacher S, Esporcatte BL, Fortes Fda S, Rocha NN, Montalvão F, Costa PC, Belem L, Rabischoffisky A, Faria Neto HC, Vasconcellos R, Iacobas DA, Iacobas S, Spray DC, Thomas NM, Goldenberg RC, de Carvalho AC. Functional and transcriptomic recovery of infarcted mouse myocardium treated with bone marrow mononuclear cells. Stem Cell Rev Rep. 2012 Mar;8(1):251-61. https://doi.org/10.1007/s12015-011-9282-2.
128. Liu, L.; Jiang, Q.; Du, C.; Yang, T.; Zhou, L.; Chen J. et al. Ankrd1 regulates endogenous cardiac regeneration in mice by modulating cyclin D1. *Eur J Pharmacol*. **2024**; 983:177005. https://doi.org/10.1016/j.ejphar.2024.177005.
129. Li, Y.; Wang, X.; Bi, Y.; Zhang, M.; Xiong, W.; Hu X. et al. SNX5-Rab11a protects against cardiac hypertrophy through regulating LRP6 membrane translocation. *J Mol Cell Cardiol*. **2024**; 194:46-58. https://doi.org/10.1016/j.yjmcc.2024.06.009.

 doi:10.20944/preprints202605.0124.v1

130. Kovacs, G.; Bartolome, S.; Denton, C.P.; Gatzoulis, M.A.; Gu, S.; Khanna, D. et al. Definition, classification and diagnosis of pulmonary hypertension. *Eur Respir J.* **2024**; 64(4):2401324. https://doi.org/10.1183/13993003.01324-2024.
131. Cao, Y.; Dong, W.; Shi, Y.; Sun, X.; Su, H.; Xie, D. et al. Conceptual Reconsideration of the Classification of Pulmonary Hypertension: From 5 Groups to 2 Groups. *JACC Asia*. **2026**: S2772-3747(26)00112-2. https://doi.org/10.1016/j.jacasi.2026.02.015.
132. Blanca-Jover, E.; Contreras-Chova, F.; Jerez-Calero, A.; Uberos-Fernandez, J.; Pérez-Lara, L. Congenital Heart Disease and Pulmonary Arterial Hypertension: Current Perspectives. *Rev Cardiovasc Med*. **2026**; 27(3):48337. https://doi.org/10.31083/RCM48337.
133. Qiu, Y.; Lyu, X.; Zhang, D.; Xu, H.; He, X.; Chen, J. et al. Gut Microbiota in Pulmonary Arterial Hypertension: Murine Models and Human Microbial Signatures, Pathogenic Mechanisms, and Emerging Therapeutic Avenues. *Compr Physiol*. **2026**; 16(1):e70094. https://doi.org/10.1002/cph4.70094.
134. Miller, D.M.; Archer, S.L.; Dunham-Snary, K.J. Preclinical models of mitochondrial dysfunction: mtDNA and nuclear-encoded regulators in diverse pathologies. *Front Aging*. **2025**; 6:1585508. https://doi.org/10.3389/fragi.2025.1585508.
135. Kris, L.P.; Dixon, D.L.; Bihari, S.; Carr, J.M. Revisiting the monocrotaline-treated rat as a model of inflammatory lung disease: COVID-19 and future pandemic threats? *Animal Model Exp Med*. **2025**; 8(10):1785-1793. https://doi.org/10.1002/ame2.70099.
136. Lv, X.; Li, J.; Wei, R.; Meng, L.; Kong, X.; Wei, K. et al. Ethyl pyruvate alleviates pulmonary arterial hypertension via PI3K-Akt signaling. *Mol Cell Biochem*. **2025**; 480(2):1045-1054. https://doi.org/10.1007/s11010-024-05020-1.
137. Stam, K.; Clauss, S.; Taverne, Y.J.H.J.; Merkus, D. Chronic Thromboembolic Pulmonary Hypertension–What Have We Learned From Large Animal Models. *Front Cardiovasc Med*. **2021**; 8:574360. https://doi.org/10.3389/fcvm.2021.574360.
138. Rainer, P.P.; Kass, D.A. Old dog, new tricks: novel cardiac targets and stress regulation by protein kinase G. *Cardiovasc Res.* **2016**; 111(2):154-62. https://doi.org/10.1093/cvr/cvw107.
139. Mathew, R.; Altura, B.T.; Altura, B.M. Strain differences in pulmonary hypertensive response to monocrotaline alkaloid and the beneficial effect of oral magnesium treatment. *Magnesium.* **1989**; 8(2):110-6. PMID: 2526910.
140. Krstic, A.M.; Jones, T.L.M.; Power, A.S.; Ward, M.L. The Monocrotaline Rat Model of Right Heart Disease Induced by Pulmonary Artery Hypertension. *Biomedicines.* **2024**; 12(9):1944. https://doi.org/10.3390/biomedicines12091944.
141. Ferrarini, G.; Canevari, M.; Azzini, V.; Agostoni, P.; Pezzuto, B.; Vignati, C. Physiological Responses to Acute Hypobaric and Normobaric Hypoxia: Differences in Maximal Exercise and Clinical Impact. *High Alt Med Biol*. **2026**: 15578682261442067. https://doi.org/10.1177/15578682261442067. Epub ahead of print.
142. McGowan, J.; Cook, J. Altitude-Induced Pulmonary Hypertension. **2026**. In: StatPearls [Internet]. Treasure Island (FL): StatPearls Publishing; 2026 Jan–. PMID: 32310385.
143. Mathew, R.; Huang, J.; Iacobas, S.; Iacobas, D.A. Pulmonary Hypertension Remodels the Genomic Fabrics of Major Functional Pathways. *Genes* **2020**, *11*, 126. https://doi.org/10.3390/genes11020126
144. Mathew, R.; Iacobas, S.; Huang, J.; Iacobas, D.A. Metabolic Deregulation in Pulmonary Hypertension. *Curr. Issues Mol. Biol.* **2023**, *45*, 4850-4874. https://doi.org/10.3390/cimb45060309
145. KEGG Pathways. Vascular smooth muscle contraction. Available online at: https://www.kegg.jp/pathway/rno04270. Accessed on March 21st, 2026.
146. `KEGG Pathway. Citrate Cycle (TCA Cycle)—Rattus Norvegicus (Rat). Available online: https://www.genome.jp/kegg-bin/show_pathway?rno00020. Aaccessed on Marcg 20th, 2026).
147. KEGG Pathway. Fructose and Manose Metabolism. Available online: https://www.genome.jp/kegg-bin/show_pathway?rno00051. Accessed on March 20th, 2026).
148. Alberti, K.G.; Zimmet, P.; Shaw, J. IDF Epidemiology Task Force Consensus Group. The metabolic syndrome--a new worldwide definition. *Lancet*. **2005**; 366(9491):1059-1062. https://doi.org/10.1016/S0140-6736(05)67402-8

 doi:10.20944/preprints202605.0124.v1

149. Lakka, H.M.; Laaksonen, D.E.; Lakka, T.A.; Niskanen, L.K.; Kumpusalo, E.; Tuomilehto J, et al. The metabolic syndrome and total and cardiovascular disease mortality in middle-aged men. *JAMA*. **2002**; 288(21):2709-2716. https://doi.org/10.1001/jama.288.21.2709
150. Ha, V.; Jayalath, V.H.; Cozma, A.I.; Mirrahimi, A.; de Souza, R.J.; Sievenpiper, J.L. Fructose-containing sugars, blood pressure, and cardiometabolic risk: a critical review. *Curr Hypertens Rep*. **2013**; 15(4):281-97. https://doi.org/10.1007/s11906-013-0364-1
151. Seneff, S.; Wainwright, G.; Mascitelli, L. Is the metabolic syndrome caused by a high fructose, and relatively low fat, low cholesterol diet? *Arch Med Sci*. **2011;** 7(1):8-20. https://doi.org/10.5114/aoms.2011.20598.
152. Ferder, L.; Ferder, M.D.; Inserra, F. The role of high fructose corn syrup in metabolic syndrome and hypertension. *Current Hypertension Research* **2010**; 12:105-112. https://doi.org/10.1007/s11906-010-0097-3
153. Dai, S.; McNeill, J.H. Fructose-induced hypertension in rats is concentration- and duration-dependent. *J Pharmacol Toxicol Methods* **1995**; 33(2):101-107. https://doi.org/10.1016/1056-8719(94)00063-a
154. Suzuki, M.; Yamamoto, D.; Suzuki, T.; Fujii, M.; Suzuki, N.; Fujishiro, M. et al. High fat and high fructose diet induced intracranial atherosclerosis and enhanced vasoconstrictor responses in non-human primate. *Life Sci* **2006**; 80(3):200-204. https://doi.org/10.1016/j.lfs.2006.09.002.
155. Stirpe, F.; Della Corte, E.; Bonetti, E.; Abbondanza, A.; Abbati, A.; De Stefano, F. Fructose-induced hyperuricaemia. *Lancet*. **1970**; 2(7686):1310-1311. https://doi.org/10.1016/s0140-6736(70)92269-5
156. Lê, K.A.; Ith, M.; Kreis, R.; Faeh, D.; Bortolotti, M.; Tran, C. et al. Fructose overconsumption causes dyslipidemia and ectopic lipid deposition in healthy subjects with and without a family history of type 2 diabetes. *Am J Clin Nutr*. **2009**; 89(6):1760-1765. https://doi.org/10.3945/ajcn.2008.27336.
157. Eickelmann, C.; Lieder, H.R.; Sturek, M.; Heusch, G.; Kleinbongard, P. Differences in vasomotor function of mesenteric arteries between Ossabaw minipigs with predisposition to metabolic syndrome and Göttingen minipigs. *Am J Physiol Heart Circ Physiol*. **2024**; 326(2):H408-H417. https://doi.org/10.1152/ajpheart.00719.2023.
158. Kehinde, S.A.; Qaisrani, Z.N.; Pattanayaiying, R.; Lin, W.P.; Lay, B.B.; Phyo, K.Y. et al. Preclinical Evidence of Curcuma longa Linn. as a Functional Food in the Management of Metabolic Syndrome: A Systematic Review and Meta-Analysis of Rodent Studies. *Biomedicines*. **2025**; 13(8):1911. https://doi.org/10.3390/biomedicines13081911.
159. Raju, S.U.; Shanmugapriyan, S.; Chakradhar, T.; Jaikumar, S.; Sayana, S.B.; Muninathan, N. Antioxidant Effects of Aqueous Bidens pilosa in Fructose-Fed Rats. *Cureus*. **2025**; 17(11):e97222. https://doi.org/10.7759/cureus.97222.
160. Niewiadomska, J.; Gajek-Marecka, A.; Gajek, J.; Noszczyk-Nowak, A. Biological Potential of Polyphenols in the Context of Metabolic Syndrome: An Analysis of Studies on Animal Models. *Biology (Basel)*. **2022**; 11(4):559. https://doi.org/10.3390/biology11040559.
161. Tvarijonaviciute, A.; Ceron, J.J.; Holden, S.L.; Cuthbertson, D.J.; Biourge, V.; Morris, P.J. et al. Obesity-related metabolic dysfunction in dogs: a comparison with human metabolic syndrome. *BMC Vet Res*. **2012**; 8:147. https://doi.org/10.1186/1746-6148-8-147.
162. Baharuddin, B. The Impact of Fructose Consumption on Human Health: Effects on Obesity, Hyperglycemia, Diabetes, Uric Acid, and Oxidative Stress With a Focus on the Liver. *Cureus*. **2024**; 16(9):e70095. https://doi.org/10.7759/cureus.70095.
163. Tappy, L.; Le, K.A. Metabolic effects of fructose and the world wide increase in obesity. *Physiol Rev* **2010**; 90(1):23-46. https://doi.org/10.1152/physrev.00019.2009
164. Kertowidjojo, E.; Iacobas, D.A. Insulin resistance and the metabolic syndrome severity—a mathematical model. *Academy of Romanian Scientists—Annals Series on biological Sciences,* **2022,** 11(1), 91-103. https://doi.org/10.56082/annalsarscibio.2022.1.91
165. Ferreira, M.D.S.; Maldonado, R.A.; Farani, P.S.G. Chagas Disease in the 21st Century: Global Spread, Ecological Shifts, and Research Frontiers. *Biology (Basel)*. **2025**; 14(11):1631. https://doi.org/10.3390/biology14111631.
166. Ying, H.; Fan, H.; Wang, Y.; Jiang, R.; Cai, D.; Cheng, H. et al. Connexin43 Deficiency Leads to Ventricular Arrhythmias by Reprogramming Proline Metabolism. *Adv Sci (Weinh)*. **2026**; 13(19):e16090. https://doi.org/10.1002/advs.202516090.

 doi:10.20944/preprints202605.0124.v1

167. Zhang, J.; Zanella, F.; Ellis, M.W.; Bradford, W.H.; Gutierrez-Lara, E.J.; Wang, T.M. et al. Connexin-43 Restoration Alleviates Desmosomal Arrhythmogenic Cardiomyopathy. *Circ Heart Fail*. **2026**; 19(4):e013801. https://doi.org/10.1161/CIRCHEARTFAILURE.125.013801.
168. Žigová, L.; Hrubá, O.; Kyselovic, J.; Gažová, A. Connexin 43 in Pathophysiology of Cardiac Diseases: From Molecular Mechanisms to Therapeutic Strategies. *Physiol Res*. **2025**; 74(6):909-921. https://doi.org/10.33549/physiolres.935633.
169. Iacobas, D.A.; Iacobas, S.; Li, W.E.; Zoidl, G.; Dermietzel, R.; Spray, D.C. Genes controlling multiple functional pathways are transcriptionally regulated in connexin43 null mouse heart. *Physiol Genomics*. **2005**; 20(3):211-23. https://doi.org/10.1152/physiolgenomics.00229.2003.
170. Ybanez, T.; Ingles, J.; Du Toit, E.; Peart, J. Cardioprotection Through Mitochondrial Modulation: A Systematic Review of Pharmacological Interventions in Animal Models of I/R Injury. *Cardiovasc Drugs Ther*. **2026** Mar 4. https://doi.org/10.1007/s10557-026-07851-0. Epub ahead of print.
171. Golforoush, P.; Yellon, D.M.; Davidson, S.M. Mouse models of atherosclerosis and their suitability for the study of myocardial infarction. *Basic Res Cardiol*. **2020**; 115(6):73. https://doi.org/10.1007/s00395-020-00829-5.
172. Bouchet, C.; Guibert, C.; Freund-Michel, V. Le facteur de croissance des nerfs (NGF) dans l'hypertension pulmonaire (HTP) [Nerve growth factor (NGF) in pulmonary hypertension (PH)]. Rev Mal Respir. 2024; 41(4):265-268. French. https://doi.org/10.1016/j.rmr.2024.02.007.
173. Ning, S.; Guo, X.; Zhu, Y.; Li, C.; Li, R.; Meng, Y. et al. The mechanism of NRF2 regulating cell proliferation and mesenchymal transformation in pulmonary hypertension. Int J Biol Macromol. 2024; 275(Pt 1):133514. https://doi.org/10.1016/j.ijbiomac.2024.133514.
174. Mani, S.; Berger, S.I. Genetic Variants Associated with Persistent Pulmonary Hypertension of Newborn: A Systematic Review. Neonatology. 2026 Mar 13:1-12. https://doi.org/10.1159/000550289. Epub ahead of print.
175. Bousseau, S.; Gu, S.; Lahm, T. Biological and Clinical Implications of Sex Differences in Right Heart Failure Associated With Pulmonary Arterial Hypertension. *Arterioscler Thromb Vasc Biol*. **2026** Apr 30. https://doi.org/10.1161/ATVBAHA.126.322096. Epub ahead of print.
176. Verkest, K.R. Is the metabolic syndrome a useful clinical concept in dogs? A review of the evidence. *Vet J*. **2014**; 199(1):24-30. https://doi.org/10.1016/j.tvjl.2013.09.057.